

Sami-Seppo Ovaska

OIL AND GREASE BARRIER PROPERTIES OF CONVERTED DISPERSION-COATED PAPERBOARDS

Thesis for the degree of Doctor of Science (Technology) to be presented with due permission for public examination and criticism in Auditorium 4301–4302 at Lappeenranta University of Technology, Lappeenranta, Finland on the 25th of November 2016 at noon.

Acta Universitatis
Lappeenrantaensis 719

Supervisor Professor Kaj Backfolk
LUT School of Energy Systems
Lappeenranta University of Technology
Finland

Reviewers Professor Caisa Johansson
Faculty of Health, Science and Technology
Karlstad University
Sweden

Professor Jurkka Kuusipalo
Department of Materials Science
Tampere University of Technology
Finland

Opponent Professor Jurkka Kuusipalo
Department of Materials Science
Tampere University of Technology
Finland

Custos Professor Kaj Backfolk

ISBN 978-952-335-008-3

ISBN 978-952-335-009-0 (PDF)

ISSN-L 1456-4491

ISSN 1456-4491

Lappeenrannan teknillinen yliopisto

Yliopistopaino 2016

ABSTRACT

Sami-Seppo Ovaska

Oil and grease barrier properties of converted dispersion-coated paperboards

Lappeenranta 2016

92 pages

Acta Universitatis Lappeenrantaensis 719

Diss. Lappeenranta University of Technology

ISBN 978-952-335-008-3, ISBN 978-952-335-009-0 (PDF),

ISSN-L 1456-4491, ISSN 1456-4491

Changes in consumer habits and the replacement of solid trans fats in foodstuffs with unsaturated fats have increased the demand for low-cost grease-resistant packaging materials worldwide. Taking into account the global aim to reduce our dependence on oil-based plastics, new bio-based solutions are needed to meet the demand for sustainable packaging solutions, and the development of such materials was the focus of the work reported in this thesis.

Pigmented dispersion barrier coatings were prepared using a blade-coating technique on commercial solid bleached sulphate paperboard. The coatings consisted of a bio-based component, hydroxypropylated starch or hydroxypropyl cellulose, a styrene-butadiene latex binder, and talc. The grease resistance in terms of time taken for a model grease to penetrate the coated paperboard varied between a few hours and several days, depending on the coating composition and on the ambient temperature during the test. Particular attention was given to coatings that prevented oil to penetrate the whole 24 h test period described in ISO 16532-1.

The feasibility of producing barrier-coated boards was studied from the viewpoints of the finishing and converting processes and their end-use applications. The findings suggested that corona treatment should be used with caution if the board is to be printed, since it may cause a drastic decrease in oil penetration time due to strike through that occur if the voltage of the discharge is sufficiently high to change the electrical conductivity of the sample. The oil barrier was impaired regardless of whether the uncoated or the coated side of the board was treated with corona. Moreover, the coatings did not prevent the occurrence of reverse side effects.

Unexpectedly, contact angle determinations suggested that exposure to heat in converting processes may even improve the oil repellency of dispersion coatings containing pigments due to the migration of latex towards the outer surface. Migrated latex also induced self-healing of the coating, according to scanning electron microscope (SEM) images that indicated the disappearance of pinholes. The oil and grease resistance (OGR) was, however, dependent on the oil viscosity and fatty acid composition. Particularly with moderately grease-resistant samples, the penetration time of pure coconut and rapeseed oils was considerably longer than that of their mixtures. Finally, press forming of paperboard led to a decrease in oil penetration time, but none of the studied coating compositions completely lost their barrier properties.

The developed coating formulations seem to have a potential in many commercial sustainable packaging applications in a transitional period before implementation of completely bio-based coatings on an industrial scale. Potential uses may include e.g. instant meal trays and fast food packages, but particular attention should be paid to the effects of converting and finishing processes on the physical and barrier properties of the materials.

Keywords: barrier properties, corona treatment, dispersion coating, oil and grease resistance

FOREWORD AND ACKNOWLEDGEMENTS

This thesis describes research that has been carried out in the research groups of Biomaterials and Packaging technology at Lappeenranta University of Technology over the period 2011–2016. A substantial part of the present work is based on projects “Future Biorefinery 2 – FuBio”, financed by Fibic Ltd., and “Tulevaisuuden turvalliset elintarvikepakkaukset” financed by The European Regional Development Fund. This study also received funding from The International Doctoral Programme in Bioproducts Technology (PaPSaT). All the funding organizations and industrial partners of the project consortia are gratefully acknowledged.

Finding the right path in the world of academic engineering is not always easy. I wish to express my gratitude to my supervisor Professor Kaj Backfolk for invaluable guidance and advice. Under his encouraging supervision, a path to follow was relatively easy to find. I also thank Professor Caisa Johansson and Professor Jurkka Kuusipalo for pre-examining the thesis. My special thanks go to Dr. J. Anthony Bristow, our trusted language consultant, whose valuable guidance I deeply appreciate. I also owe thanks to Professor Thad Maloney, the program director of PaPSaT, and the whole PaPSaT board, who gave me a unique opportunity to be a part of this traditional graduate school.

My current and former colleagues at both the research groups are gratefully acknowledged for practical help and intellectual support. In spite of numerous smaller or larger setbacks and challenges we faced during the shared years, the team spirit remained high. Especially, Dr. Katriina Mielonen, thank you for all our serious and less serious conversations, and your advice and support. I also thank Mr. Antti T. Karhu for his valuable contribution in the laboratory.

Finally, I am grateful to my parents Helena and Seppo and my life companion Minna for all the support I have received.

“Anyone who stops learning is old, whether at twenty or eighty. Anyone who keeps learning stays young.” (Henry Ford)

Lappeenranta, November 2016

Sami-Seppo Ovaska

LIST OF PUBLICATIONS

The thesis consists of a theoretical introduction and summary of the publications listed below

- I. Ovaska, S.-S., Geydt, P., Österberg, M., Johansson, L.-S., Backfolk, K. (2015). Heat-Induced Changes in Oil and Grease Resistant Hydroxypropylated-Starch-Based Barrier Coatings, *Nord. Pulp Paper Res. J.*, 30 (3), pp. 488–496.
- II. Ovaska, S.-S., Hiltunen, S., Erntsson, M., Schuster, E., Altskär, A., Backfolk, K. (2016). Characterization of Rapeseed Oil/Coconut Oil Mixtures and Their Penetration into Hydroxypropylated-Starch-Based Barrier Coatings Containing an Oleophilic Mineral, *Prog. Org. Coat.*, 101, 569–576.
- III. Ovaska, S.-S., Mielonen, K., Lozovski, T., Rinkunas, R., Sidaravicius, J., Backfolk, K. (2015). A novel approach for studying the effects of corona treatment on ink-substrate interactions, *Nord. Pulp Paper Res. J.*, 30 (4), pp. 681–688.
- IV. Ovaska, S.-S., Geydt, P., Rinkunas, R., Lozovski, T., Maldzius, R., Sidaravicius, J., Österberg, M., Johansson, L.-S., Backfolk, K. (2016). Corona treatment of filled dual-polymer dispersion coatings: Surface properties and grease resistance, accepted for publication in *Polym. Polym. Compos.* in March 2016.
- V. Ovaska, S.-S., Rinkunas, R., Lozovski, T., Maldzius, R., Sidaravicius, J., Johansson, L.-S., Österberg, M., Backfolk, K. (2016). Occurrence of reverse side effects in corona treatment of dispersion-coated paperboard and its influence on grease barrier properties, *J. Appl. Packag. Res.*, 8 (3), pp. 68–79.
- VI. Leminen, V., Ovaska, S.-S., Tanninen, P., Varis, J. (2015). Convertability and Oil Resistance of Paperboard with Hydroxypropyl-Cellulose-Based Dispersion Barrier Coatings, *J. Appl. Packag. Res.*, 7 (3), pp. 91–100.

AUTHOR'S CONTRIBUTION TO THE WORK PRESENTED IN THE LISTED PUBLICATIONS

- I. Planning the trials and development of the coating recipes. Testing of the coated samples excluding the AFM and XPS measurements. Interpretation of all results, and writing the manuscript with co-authors.

- II. Planning the experimental setup and interpretation of the results. Testing oil and grease resistance. Writing the manuscript with co-authors.
- III. Laboratory testing of samples with the exception of the corona treatment. Analyzing all the results. Writing the manuscript with co-authors.
- IV. Planning the experiments, testing the corona-treated samples and interpretation of the results. Writing the manuscript with co-authors.
- V. Planning the experiments, testing the corona-treated samples and interpretation of the results. Writing the manuscript with co-authors.
- VI. Development of coating recipes and testing of coated samples excluding converting trials. Interpretation of the results related to coatings and barrier properties. Writing the manuscript with co-authors.

SUPPORTING PUBLICATIONS

- SI. Ovaska, S.-S., Backfolk, K. (2013). Optimizing grease resistance of dispersion barrier coatings for heterogeneous grease mixtures. 26th PTS Coating Symposium. Munich, Germany. PTS – ST 1301, pp. 411–423.
- SII. Ovaska S.-S., Mielonen, K., Saukkonen, E., Lozovski, T., Rinkunas, R., Sidaravicius, J., Backfolk, K. (2014). A Novel Method to Study the Effect of Corona Treatment on Ink Wetting and Sorption Behavior. 30th International Conference on Digital Printing Technologies. Philadelphia, PA, USA. IS&T, Springfield, VA, USA, pp. 362–365.
- SIII. Mielonen, K., Ovaska, S.-S., Backfolk, K. (2015). Potential of Coating Comprising Hydroxypropylated Starch for Dye-Based Inkjet Printing. 31th International Conference on Digital Printing Technologies. Portland, OR, USA. IS&T, Springfield, VA, USA, pp. 357–361.
- SIV. Koivula, H., Jalkanen, L., Saukkonen, E., Ovaska, S.-S., Lahti, J., Christophliemk, H., Mikkonen, K. S. (2016). Machine-coated starch-based dispersion coatings prevent mineral oil migration from paperboard, *Prog. Org. Coat.*, 99, pp. 173–181.
- SV. Leminen, V., Ovaska, S.-S., Wallmeier, M., Hauptmann, M., Backfolk, K., Varis, J. (2016). Effect of material properties and drawing parameters on the quality of deep-drawn paperboard products. 26th International Conference on Flexible Automation and Intelligent Manufacturing. Seoul, Republic of Korea. 8 p.

ABBREVIATIONS

AFM	Atomic force microscopy
AKD	Alkylketene dimer
BAA	Bristow absorption apparatus
CLSM	Confocal laser scanning microscopy
CMC	Carboxymethyl cellulose
CPVC	Critical pigment volume concentration
CT	Corona treatment
DIM	Diiodomethane
EG	Ethylene glycol
FRAP	Fluorescence recovery after photobleaching
GCC	Ground calcium carbonate
HPC	Hydroxypropyl cellulose
HPS	Hydroxypropylated starch
MFC	Microfibrillated cellulose
MFFT	Minimum film formation temperature
n.m.	Not measured
OGR	Oil and grease resistance
OTR	Oxygen transmission rate
PET	Polyethylene terephthalate
PVA	Poly(vinyl alcohol)
RMS	Root mean square
SA	Styrene-acrylate
SB	Styrene-butadiene
SBS	Solid bleached sulphate
SEM	Scanning electron microscopy
SFE	Surface free energy
T _g	Glass transition temperature
WVTR	Water vapor transmission rate
XPS	X-ray photoelectron spectroscopy

TABLE OF CONTENTS

1 INTRODUCTION.....	13
1.1 Background.....	13
1.2 Objective of the study.....	15
1.3 Outline	16
2 DISPERSION BARRIER COATING	17
2.1 Formulation of coating dispersions	17
2.1.1 Synthetic polymer dispersions.....	17
2.1.2 Biopolymer-synthetic polymer systems.....	18
2.1.3 Pigmented polymer dispersion barrier coatings	19
2.2 Coating methods.....	21
2.3 Drying and film formation.....	23
2.4 Limiting factors for implementing dispersion coating	24
3 BASIC PRINCIPLES OF INTERACTIONS BETWEEN A LIQUID AND A SUBSTRATE.....	27
3.1 Fundamentals of absorption and wetting	27
3.2 Liquid penetration into fiber-based substrates	28
3.3 Effect of surface roughness and liquid viscosity.....	30
4 OIL AND GREASE RESISTANCE	33
4.1 Oil repellence – physico-chemical approach.....	33
4.2 Oil resistance – physical barrier	34
4.3 Effect of base substrate on oil penetration.....	35
4.4 Effect of fatty acid composition on oil penetration.....	35
5 OIL AND GREASE BARRIER PROPERTIES OF CONVERTED PAPERS AND BOARDS.....	37
5.1 Fundamentals of surface treatment of fiber-based substrates with corona.....	37
5.2 Over-treatment and reverse-side effects	38
5.3 Effect of corona treatment on barrier properties	39
5.4 Effects of mechanical converting on the barrier properties of biopolymer-coated paperboards	40
EXPERIMENTAL	43
6 MATERIALS AND METHODS	43

6.1	Coating process and substrate	43
6.2	Coating dispersions	44
6.3	Corona treatment and chemical composition of coated surfaces	45
6.3.1	Design of the corona treatment apparatus.....	45
6.3.2	Chemical analysis of the surfaces.....	45
6.4	Preparation of oil blends and their characterization.....	46
6.5	Contact angle and surface free energy determinations.....	46
6.6	Imaging methods.....	47
6.6.1	Coating coverage and study of sealing surfaces.....	47
6.6.2	Physico-chemical analyses with an atomic force microscope	47
6.6.3	Oil penetration studies with a confocal laser scanning microscope	48
6.7	Oil and grease resistance	48
7	RESULTS AND DISCUSSION	51
7.1	Oil and grease resistance of non-converted boards (Papers I-II).....	51
7.1.1	Effect of ambient temperature on oil penetration time	51
7.1.2	Effect of oil fatty acid composition on oil penetration time and behavior	53
7.1.3	Cross-sectional analysis of oil diffusion into dispersion-coated board	55
7.2	Effect of electrical treatment on oil-substrate interactions (Papers III-V)	57
7.2.1	Corona-treated dispersion barrier coatings	57
7.2.2	Reverse-side phenomena.....	64
7.2.3	Conclusions of the oil and grease resistance of corona-treated substrates	68
7.3	Effect of heat exposure and high ambient temperature on coating properties and on oil-substrate interactions (Papers I and VI).....	69
7.3.1	Effect of heat on the chemical composition of coated surfaces	69
7.3.2	Physico-chemical properties of dispersion coatings.....	70
7.3.3	Interactions between substrate and rapeseed oil at elevated temperatures	75
7.4	Oil and grease resistance after mechanical processing of paperboard (Paper VI).....	77
7.4.1	Effect of gelatin on the post-creasing OGR of HPS- and HPC-based coatings.	78
7.4.2	OGR of press-formed trays	78
8	CONCLUDING REMARKS	81
	REFERENCES.....	83

1 INTRODUCTION

1.1 Background

It has been predicted that the global packaging market will reach \$820 billion by 2016, and the total functional- and barrier-coated paper and paperboard market was \$3.9 billion in 2010. Almost two thirds of this value originated from products coated with extrusion polymers or aluminium (Harrod 2011). However, increasing environmental concerns over the use of non-renewable oil-based polymers in packaging materials have increased the general interest in using renewable coating components. At the same time, consumer habits have changed worldwide (Anon. 2006), and the demands for cost reduction and a wider utilization of sustainable packaging materials require new barrier solutions especially for short-term uses. Examples of such food products are bakery goods, microwavable instant meals and fast foods.

The main purpose of the food package is to protect the packed food from outer substances or threats that are considered harmful to the food. Contamination by dirt, gases, migration, aromas, UV radiation, odors and water should be minimized. Besides protecting food from outer threats, the package must also retain the components of the packed food inside the package. Oil and grease resistance is thus an essential material property, and it can also prolong the shelf-life and maintain the quality of the food (Zhao and McDaniel 2005), e.g. by decreasing the aroma loss of packed foodstuff (Fayoux et al. 1997; Hernandez-Muñoz et al. 1999), and its significance can be assumed to increase further due to an increasing consumption of fast food and convenience meals.

Vegetable parchment paper, which was invented in the 1850s (Gaine 1853), can be considered to be the first fiber-based material with grease-barrier properties but it took few decades before the barrier properties of greaseproof papers were improved by coatings (Staples et al. 1899). The implementation of aqueous coatings began to spread in the middle of the 20th century. In the 1950s, synthetic polymer dispersions were used to decrease the water vapor transmission rate of cellophane (Bristow 2016), and the evolvement of dispersion coating techniques for coating paper or paperboard has been relatively rapid in recent decades (Figure 1.1). Unlike extrusion-coated or plastic-laminated materials, dispersion-coated papers and boards can be repulped or composted (Kimpimäki and Savolainen 1997). Alternatively, dispersion-coated materials can be burned at a waste burning plant like plastic packages. This indicates that

dispersion coating has certain environmental benefits over plastic coatings. In addition, dispersion coating can be carried out as an online process. The first generation of coating dispersions was based on aqueous synthetic polymers, such as hydrocarbon resins for improving waterproofness (Powers and Pflum 1961) and polyolefin dispersions for improving e.g. grease and gas barrier properties (Sculley and Bruno 1968). The development has been rapid. The water vapor barrier properties of the latex-based dispersion coatings can for instance be improved by e.g. the addition of wax (Schumann et al. 2005a) or plate-like fillers such as kaolin (Zhu et al. 2013). Examples of other advances are the partial replacement of synthetic polymers with bio-based alternatives, such as modified starches (Jansson 2006; Tanninen et al. 2014), and a synthetic-polymer-free combination of starch-plasticizer solution with montmorillonite clay (Olsson et al. 2014a). Recent findings have also shown that dispersion barrier coatings can be tailored for printing applications (Mielonen et al. 2015) and that they prevent the migration of mineral oil well (Koivula et al. 2016).

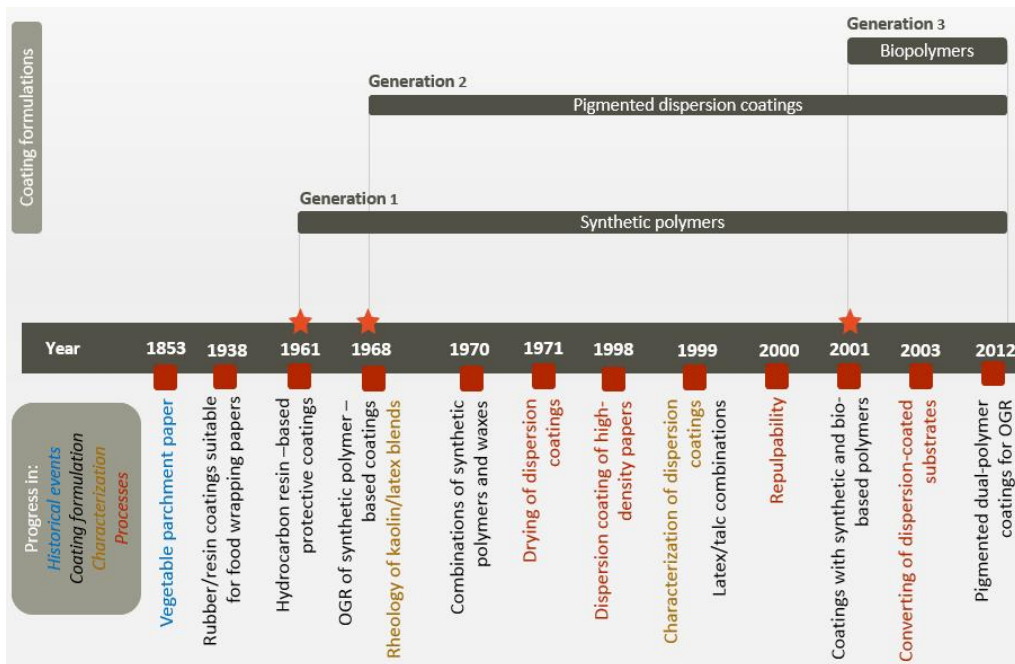


Figure 1.1 The evolution of dispersion coatings based on a Scopus database search and a patent search. (Gaine 1853; Elliot 1938; Powers and Pflum 1961; Sculley and Bruno 1968; Csuros et al. 1968; Black et al. 1970; Smirnova et al. 1971; Vähä-Nissi et al. 1998a; Rissa et al. 1999; Vähä-Nissi and Savolainen 1999; Vähä-Nissi et al. 2000; Vähä-Nissi et al. 2001; Kuusipalo 2003; Karhu 2012)

There is indeed a substantial amount of literature related to the formulation of barrier dispersions and barrier properties of dispersion coatings. However, the oil and grease resistance of dispersion barrier coatings has usually been studied by standard methods, which may describe the real-life end-use insufficiently. There is an obvious need to understand the effects of converting and finishing processes on the barrier properties of dispersion-coated substrates, and on their printability or end-use usability, all of which are essential for successful commercial applications.

1.2 Objective of the study

The objective of this work was to investigate the oil repellence and resistance of dispersion-coated paperboard from the viewpoints of converting and finishing processes and the end-use. During these processes, the substrate is exposed to e.g. electrical discharges, thermal treatment and mechanical forces such as pressure. The particular emphasis in this work has been on the partial replacing of synthetic polymers in the coatings with bio-based alternatives, and on studying the convertability of the coated substrate. The dispersion coating recipes have represented a *dual-polymer approach*, consisting of polymeric components with the addition of an inorganic mineral. In dispersion coating, high multi-barrier properties can be obtained, but the open questions are related to the formulation of the coating dispersion, i.e. finding the optimal pigment content and an optimal ratio of the biopolymer to the synthetic polymer in the dispersion. Since the coalescence of biopolymers and latices in coatings is very different, the utilization of a highly bio-based coating dispersion is considered difficult, but it was assumed that the functionality of the dual-polymer coating could be improved by the addition of a pigment. To test this hypothesis, the oil resistance of several experimental dispersion-coated paperboards was determined using a standard test method.

Standard test methods for oil resistance, however, describe the true end-use inadequately. Very often, the packed food contains several different types of oils, and this means that it is necessary to examine the situation in a wider perspective. Therefore, the effect of the saturated fatty acid content on the oil penetration time was investigated by replacing the standard oil (palm kernel oil) with mixtures of coconut oil (contains > 90% saturated fatty acids) and rapeseed oil (contains > 90% unsaturated fatty acids). Bearing in mind that the paperboard experiences several converting and finishing processes before it is used as a package, the effects of corona treatment and heat exposure on the oil repellence and oil resistance were investigated. Corona

treatment is widely-used in many printing processes to alter the wetting kinetics, but it can also be used to improve the adhesion of a polymeric coating. To adjust the treatment level accurately and to increase the flexibility of the experimental setup, a novel test method based on a modification of the Bristow Absorption Apparatus (BAA) was developed to reveal information about the influence of corona discharge on oil-substrate interactions and also on reverse-side effects. Furthermore, since the substrate is exposed to heat in many converting processes such as press-forming, heat-induced changes occurring in dry dispersion coatings were evaluated by measuring the contact angles of rapeseed oil on the board after heat treatments, and by determining the chemical composition of the coated surfaces before and after heat exposure with X-ray photoelectron spectroscopy (XPS), and by imaging *in-situ* with an atomic force microscope (AFM) the changes occurring in the coatings at different temperatures. All above-mentioned measurement techniques together made it possible to discuss the whole value chain beginning from designing the coating recipes and dispersion coating process to end-use phase of food packages.

1.3 Outline

The experimental part and Papers I–VI give the details of the work carried out. These papers discuss the factors that affect the oil and grease resistance of hydroxypropylated starch-based dispersion coatings filled with talc (Papers I–II, IV–V), the effects of heat exposure in the coating layer (Paper I), the influence of corona treatment (Papers III–V), and the post-converting grease resistance of paperboard coated with hydroxypropyl-cellulose-based dispersions (Paper VI). The experimental part of the thesis also contains a few earlier unpublished results.

2 DISPERSION BARRIER COATING

A dispersion is a system of dispersed particles suspended in a matrix, which can be solid, liquid, or gas. Dispersion coating refers here to the application onto a fiber-based web of a waterborne coating with a high proportion of polymeric substances using a conventional coating method such as blade coating. The dispersion formulations may include synthetic and bio-based polymers, inorganic minerals and additives such as biocides and anti-foaming agents. A simplified chart of a polymer dispersion-coating process (Fig. 2.1) shows the process and it resembles substantially a pigment-coating process, but it includes several events that have a crucial influence on the formation of a uniform film, and on the barrier properties of the coated substrate (Kimpimäki 1998). This chapter describes the major measures that can be adopted to optimize the quality and maximize the oil- and grease-barrier properties of the dispersion-coated board.

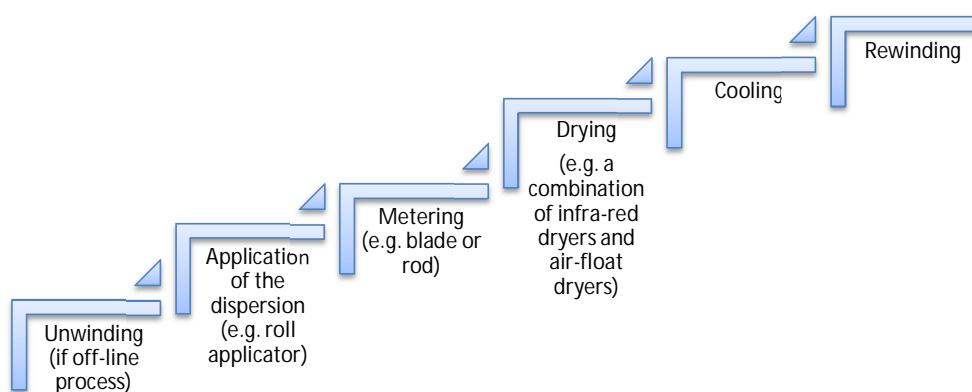


Figure 2.1 Simplified phases of a dispersion-coating process.

2.1 Formulation of coating dispersions

2.1.1 Synthetic polymer dispersions

The simplest dispersion coatings are plain aqueous dispersions of a synthetic polymer. However, several dispersion-related factors having an influence on the mechanical and barrier

properties of the synthetic-polymer-based coating have been recognized. In the case of styrene-butadiene (SB) latices, for example, the degree of cross-linking, the minimum film formation temperature and the glass transition temperature (T_g) of the polymer are the main factors that affect the mechanical properties of the film. A high degree of cross-linking increases e.g. the strain at break and work at rupture of the latex film, but it has also been suggested that highly cross-linked latices form less homogeneous films and hence tend to block more easily (Schumann et al. 2004a). A less homogeneous film does not, however, necessarily mean impaired barrier properties in the case of a highly cross-linked latex. Moreover, a low glass transition temperature may cause blocking and sticking problems, but the undeniable benefit of a low T_g latex is its lesser cracking tendency, which is crucial from the barrier point of view (Schumann et al. 2004a; Bollström et al. 2013). A low T_g also increases the interactions with both mineral and vegetable oils (Rousu et al. 2002). The addition of paraffin wax has been reported to reduce the blocking tendency of latex dispersion coatings and to decrease the WVTR effectively (Schumann et al. 2004b).

2.1.2 *Biopolymer-synthetic polymer systems*

An increasing environmental awareness has speeded up the wider utilization of biopolymers, and this can also be seen in the recent advances in dispersion coating. Hydroxypropylated starch has been successfully investigated as a replacement for the copolymer dispersion of acrylic ester, styrene and acrylonitrile from the grease-barrier point of view by Tanninen et al. (2014). An increase in the proportion of starch led, however, to an increase in the curling tendency of the coated paperboard. It was also found that a small proportion of synthetic polymer in the coating improves the convertability of the coated board in a press forming process and that the addition of kaolin had no major influence on the convertability. The oil and grease resistance of the coated boards was dependent on the coat weight, but surprisingly, above a certain coat weight a higher coat weight did not provide a better grease barrier. This might be due to poorer coalescence of the coating, since the film formation process of a synthetic, non-cross-linked polymer differs substantially from that of gel-like starch, which forms a film even at room temperature and whose film formation speed is more or less dependent on ambient temperature. It has also been suggested that a high coating layer thickness impairs the orientation of the pigment in the dispersion coating layer (Rissa et al. 2000), and that this leads to poorer barrier properties. Compatibility problems between hydrophilic and hydrophobic polymer dispersions may explain the poorer barrier properties with higher coat weights reported by Tanninen et al.

(2014). In pigment coating, the compatibility problems between synthetic binders and bio-based binders are well-known, and it has been suggested that 30–50% of the synthetic latex can be replaced without risking the runnability and performance (Oberndorfer and Greenall 2011), but there is a lack of literature about the use of bio-based binders in dispersion coating.

According to the literature, hydroxypropylated starch has some potential in dispersion-barrier-coating applications. Hydroxypropylation of starch lowers the oxygen permeability (Roth and Mehlretter 1967), and also yields more flexible films than other types of commonly used starches (Tuschhoff 1986). Typically, starch cannot be used without a plasticizer (Mali et al. 2005), and several potential plasticizers for starch have been proposed. For instance, Olsson et al. (2014b) studied hydroxypropylated starch-based barrier dispersion coatings plasticized with citric acid with and without the addition of nanoclay. The results showed that the combination of citric acid and hydroxypropylated starch leads to a low WVTR, probably due to a cross-linking reaction, but citric acid impairs the barrier properties if nanoclay is present in the coating. In that case, citric acid should be replaced with poly(ethylene glycol) in order to maintain a low WVTR.

Bearing in mind that synthetic latex can be partially replaced with a bio-based latex (Bloembergen et al. 2014) or other biopolymer dispersions (Vähä-Nissi et al. 2011) in pigment coating applications, it can be expected that the proportion of bio-based components will also be increased in barrier coating applications in the future. Combining dispersion and extrusion coatings is another possible future prospect. A recent investigation (Olsson et al. 2014a) showed that hydroxypropylated-starch-based coatings filled with nanoclay provide competitive multi-barrier properties and that by coating the dispersion coating layer with extruded polyethylene, the oxygen transmission rate (OTR) can also be reduced.

2.1.3 Pigmented polymer dispersion barrier coatings

Introducing a mineral filler into the synthetic polymer dispersion improves the runnability of the coating process, significantly reduces the blocking tendency of the coatings, and ideally reduces raw material costs without compromising the barrier properties of the coated paperboard (Vähä-Nissi and Savolainen 1999; Bollström et al. 2013). An improvement in the water vapor barrier properties can be achieved by using a plate-like minerals such as kaolin or talc together with SB-latex or poly(vinyl alcohol) (PVA), but nanoclay-PVA coatings also

provide a low WVTR (Schumann et al. 2005b). The improvement is based on the tortuous structure of the coating layer, lengthening the pathway for penetrants (Zhu et al. 2013), but the ability of the coating components to absorb oil must also be taken into account, since high oil absorption improves the oil and grease resistance, and this favors the use of oleophilic pigments such as talc (Morabito 2004). However, the component that defines the barrier properties of the dispersion-coated substrate is the polymer component. For instance, a less porous coating can be obtained by using an anionic SB-latex instead of a weakly cationic dispersion (Finch 2001). Bollström et al. (2013) compared the barrier properties of kaolin-filled styrene-acrylate (SA) latex, SB-latex, and ethylene acrylic latex, and observed that the addition of kaolin clearly reduced the WVTR of SA-latex-coated paper, but that the effect of kaolin was not as pronounced in the presence of SB-latex or ethylene acrylic latex. A pure ethylene acrylic latex coating was superior to a SA-latex coating as a water vapor barrier. Dual-polymer systems consisting of a synthetic polymer dispersion and hydroxypropylated starch can also be pigmented with kaolin without compromising the grease barrier properties (Tanninen et al. 2014).

When formulating a pigmented coating dispersion recipe, the pigment-dependent critical pigment volume concentration (CPVC) must be taken into account. CPVC is the maximum concentration of pigment by volume in an aqueous polymer dispersion at which the voids between the pigment particles remain filled with a polymer dispersion. For instance, a lower CPVC level has been reported for spherical pigments such as ground calcium carbonate (GCC) than plate-like pigments such as talc, probably due to flocculation of GCC (Vähä-Nissi and Savolainen 1999). On the other hand, a small particle size and low shape factor of the pigment assists in the formation of a densely packed structure, and theoretically this should lead to a higher CPVC. The results of Bollström et al. (2013) indicate that the CPVC of GCC is almost 20% higher than that of barrier-grade kaolin clay. It is thus evident that the CPVC should be determined for each pigment to be used as an additive in a coating dispersion in order to obtain a smooth film. Furthermore, the particle shape is an important property affecting the efficiency of the barrier dispersion coating. Despite the fact that spherical GCC has a better resistance to strong folding with *low* pigmentation levels, the grease resistance of a dispersion coating containing kaolin or talc is better on a flat or slightly folded surface. Calcinated kaolin, however, results in a bulky coating with a low grease resistance (Vähä-Nissi and Savolainen 1999).

There is evidence that the particle size distribution of the pigment has very little influence on the barrier properties of a latex/pigment coating, despite the fact that an increase in pigment concentration reduces the proportion of oil-soluble components in the coatings. Zhu et al. (2013) found that the barrier properties are dominated mainly by the aspect ratio and the disorientation of the pigment platelets in the coating, and this finding supports the utilization of large particles with a high aspect ratio in order to obtain good barrier properties. Pigment disorientation seems to reduce the tortuosity, and it can be concluded that a key to good barrier properties is maximized tortuosity.

Finally, the role of dispersants originating from the pigment should not be forgotten. It is widely known that the migration of surfactants may cause pinholes and irregularities in the coating layers in a film-forming process (Andersson et al. 2002a) and that sodium-polyacrylate-based dispersants may cause an uneven spreading of latex films (Näsman 2000), but in the case of dispersion barrier coatings the role of surfactants should be examined as a unity. There is evidence that the WVTR of dispersion-coated paperboard increases slightly with high pigmentation levels, which correlates with the surfactant content, but the presence of a surfactant may also improve the grease barrier properties of the coated product (Vähä-Nissi and Savolainen 1999).

2.2 Coating methods

An even coating thickness has typically been considered to result in good barrier properties, and this favors the use of an air knife or curtain coater instead of the more common blade or rod coater (Kimpimäki 1998). A blade-coated and an air-knife-doctored coating layer are shown in Figure 2.2. However, in numerous recent publications, pilot-scale blade coaters have been successfully used to produce barriers from latex-based systems (Schumann et al. 2005b) and even from hydroxypropylated-starch-based dispersions (Olsson et al. 2014a; Tanninen et al. 2014). The use of grooved (Rissa et al. 2000; Vähä-Nissi et al. 2006) and wire-wound rods (Andersson et al. 2002b) for barrier dispersions consisting of synthetic polymers and plate-like fillers has also been reported. In the pilot-scale manufacture of substrates for functional materials, curtain and reverse gravure coating methods have been used (Bollström et al. 2013).



Figure 2.2 The difference between a blade-coated and air-knife-coated surface. Film and rod coating methods provide a compromise between an even surface and a constant thickness. (Redrawn and modified from Kimpimäki 1998)

There thus appears to be a lot of interest in using the most conventional coating techniques such as blade and rod for applying a dispersion onto a substrate, but the coatings applied by different methods have their own unique characteristics. In addition, the presence of pigments affects the result. The orientation of pigments affects the barrier properties of a dispersion coating, and this can be studied by e.g. an X-ray diffraction technique (Rissa et al. 2000). Better orientation can be obtained by reducing the thickness of the coating layer, which indicates that multi-layering of barrier coatings provides better barrier properties than applying a single thick layer. In the field of pigment coating, Salminen et al. (2010) and Endres and Tietz (2007) have evaluated the effects of different coating methods on the structure of the coating layer, and their results indicated that the choice of coating method has a crucial effect on the structure of the coating layer. Although good coverage and a uniform coat weight can be obtained with curtain coating, the orientation of plate-like fillers is poor and the coated surface replicates the substrate roughness. Poor orientation results in a porous coating layer that is not optimal for barrier applications due to its low tortuosity, and this supports the use of conventional rod and blade coaters instead of non-impact coating methods for dispersion coating. On the other hand, spherical particles may pack densely even if a curtain method is used. The pigment shape, however, has only a minor effect on the surface smoothness if a blade coater is used (Salminen 2010).

The effects of coating method and coating composition have earlier been studied from the viewpoint of paperboard glueability in box manufacturing. Ninness et al. (2011) studied the setting of an aqueous glue on double-coated paperboard that was coated by several different coating methods, and found that the system by which the pre-coating layer was applied had a substantial influence on the setting of the adhesive. They also noticed that pigment coatings metered by a blade were less porous than film-coated or air-knife-coated coatings, but that the lower porosity did not provide a barrier to the aqueous glue. By taking also the glue penetration into account, the thickness of the applied glue layer was 141–145 μm on substrates that were

pre-coated with a blade or a rod, but only 61–81 μm if the topmost pigment coating layer was coated with an air knife. This indicates that the porosity of the coating layer is not an important parameter affecting the penetration of an aqueous glue, and emphasizes the importance of coating layer thickness, the smoothness of the coating layer, and the volume of capillary pores (discussed in detail in Chapter 3.1).

2.3 Drying and film formation

Dispersion coatings can be dried by several methods, such as infra-red dryers, air float dryers and impingement dryers. During drying, the temperature of the substrate rises typically to 80–130°C, but for latices a crucial factor is the minimum film formation temperature (MFFT) (Kimpimäki 1998), the temperature at which the polymer particles are able to form a continuous film via coalescence, which is essential for the barrier properties. The MFFT depends on the particle size, on T_g , and on the degree of cross-linking of the polymer. The presence of non-ionic surfactants may also promote the film forming of latices (Backfolk et al. 2006), whereas the segregation of anionic surfactants disturbs the film forming. Cross-linked polymers have a higher MFFT than non-cross-linked polymers such as latices (Kimpimäki 1998), suggesting that more drying capacity is needed if a dispersion containing a biopolymer is used. This is partly due to typically higher water content of dissolved biopolymers: the water content of a latex dispersion is typically approx. 50%, whereas a starch solution may contain 70–90% water. Furthermore, the film formation behavior of starch differs from synthetic polymers. The speed of film formation can be increased by increasing the drying temperature, which accelerates the evaporation of water. However, too rapid evaporation may result in blistering of the film, which destroys its barrier properties.

The wet coating layer undergoes significant transformations during the drying process. During drying, the water evaporates from the coating layer, leading to packing of the dry matter, coalescence of synthetic polymers such as latices then results in a honeycomb-like structure, and infrared dryers assist the fusion of the polymers into a homogeneous film. This yields improved barrier properties (Andersson 2001) and also improves the mechanical properties (Sababi et al. 2012) of the latex films. However, the situation is not that simple in the case of a pigmented dispersion. Binder migration in a clay-starch coating is low when the coated paper is dried at room temperature, but hot air impingement drying increases the migration of starch towards the outer surface (Dappen 1950). The movement of latex towards the base paper has

been shown to increase the proportion of pigment on the surface of the substrate (Kenttä et al. 2006), and the narrower the particle size distribution of the pigment the more latex depletion takes place (Al-Turaif and Bousfield 2005). The coating layer homogeneity can be further achieved by e.g. pre-coating and calendering (Rissa et al. 2000; Schumann et al. 2004b), i.e. to give a smoother substrate.

Due to the adhesive nature of a polymeric dispersion coating, blocking of the coated product may occur if the web temperature is too high after the drying phase, which means that the coated web should be cooled before rewinding or stacking. Synthetic polymers with a low T_g are particularly challenging with regard to blocking, but the degree of cross-linking or the presence of functional groups may also affect the blocking tendency of the dispersion-coated board (Schumann et al. 2004a). Cooling can be carried out by e.g. air cooling or cooling cylinders placed on each side of the web. It has been suggested that the cooling equipment should lower the temperature of the coated substrate to 40°C or lower, in order to reduce blocking (Ronka 2010).

2.4 Limiting factors for implementing dispersion coating

Factors that limit the use of dispersion coating can be divided into factors related to the coating dispersion, factors related to the substrate or factors related to the coating process (Figure 2.3). Skin formation takes place with latices (Steward et al. 2000), but with bio-based polymers such as starches and cellulose derivatives the rheological problems are greater. These can be reduced by decreasing the dry solids content of the coating dispersion. This increases the consumption of drying energy and makes it difficult to achieve a high coat weight with a single coating layer, and thus directs towards using pigmented coating dispersions. High viscosity also increases air entrapment (Kimpimäki 1998), which may cause pinholes in the coating layer. In order to obtain a smooth coating layer, it is important to optimize the pigment content in order to avoid water retention problems and excessive streaking. The dynamic water retention of a pigment coating containing a synthetic latex binder can be improved by introducing a starch-based binder in the recipe, but this approach may lead to depletion flocculation of pigment and latex particles if the starch/latex ratio is not optimal (Bloembergen et al. 2014).

The effect of substrate properties on the quality and runnability of a dispersion coating layer cannot be ignored. Porous substrates tend to absorb the dispersion, which complicates the film

forming and may lead to a variation in thickness of the coating layer. Minor penetration of the dispersion into the substrate may be beneficial if the substrate itself has barrier properties (Kimpimäki 1998), but the principal target must be the formation of an even coating layer if a barrier material is to be produced. Finally, the coating process should be selected carefully. The effect of the coating method on the structure of the coating layer has been discussed in detail in Chapter 2.2, but factors such as the poor performance of the air knife set speed limitations in pigmented dual-polymer systems (Finch 2001). Typical quality problems originating in the coating process are drying-related blocking and blistering. The coated web must be sufficiently dry to avoid blocking problems but too rapid drying may result in blistering e.g. in pigmented dual-polymer coatings (Karhu 2012), and this problem may be greater if the adhesion of the coating to the substrate is poor. The occurrence of blistering can also be reduced by using a more porous substrate, which allows the evaporated water to exit rapidly from the uncoated side (Vishtal and Retulainen 2012), but most importantly the coalescence of disperse phase should not begin before the water has been evaporated (Bristow 2016).

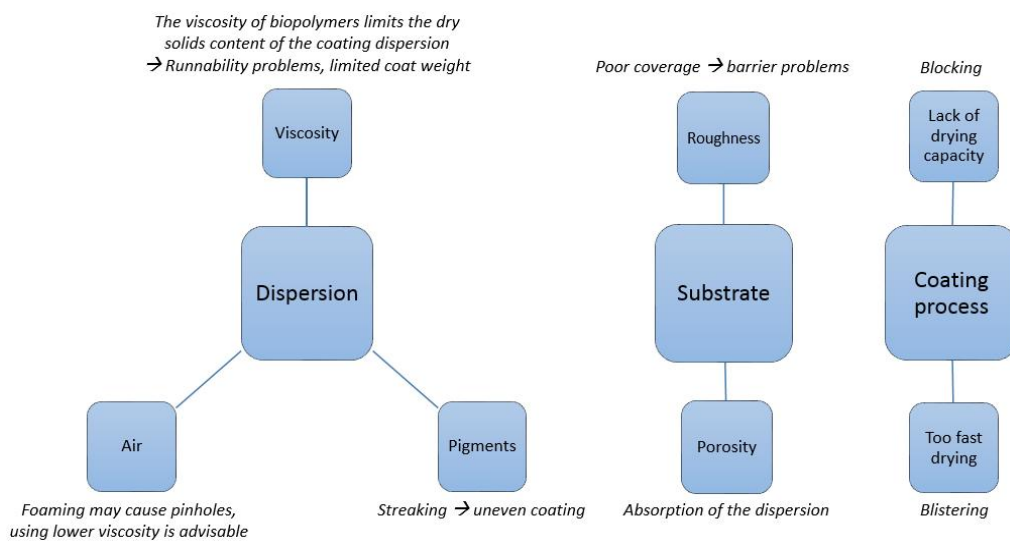


Figure 2.3 Typical factors limiting dispersion coating.

3 BASIC PRINCIPLES OF INTERACTIONS BETWEEN A LIQUID AND A SUBSTRATE

In the production of oil resistant and repellent coatings, the basic phenomena of wetting and absorption should be taken into account. The surface roughness and surface energy of the substrate are the main variables that affect the liquid spreading and wetting kinetics. The first models that describe wetting-related phenomena are designed for ideal surfaces, but the heterogeneous composition and roughness of fiber-based products mean that the basic models are inadequate. These products often have a complex porous structure, which can be described as a network of randomly distributed capillaries. The basic requisite for wetting is that the liquid spreads over the entire surface. Wetting always occurs when the contact angle is less than 90° (Figure 3.1), and the force balance between adhesive and cohesive forces determine the wettability of a material. Strong adhesion and weak cohesion are required for a low surface tension and small contact angle, leading to rapid wetting. In addition, the difference in solubility parameter between the liquid and the coating affects the liquid-substrate interaction, as in the case of biopolymers that may dissolve in edible oils.

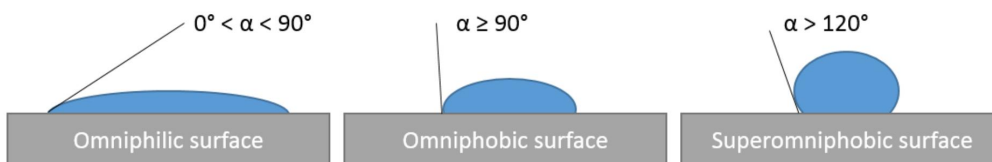


Figure 3.1 The adhesive forces between the liquid and the surface determine the liquid contact angle and the contact surface area. A liquid drop spreads out to increase the contact surface on an omniphilic surface, but on an omniphobic surface (i.e. surface repels both polar and apolar liquids), the droplet contracts and the contact area with the substrate decreases.

3.1 Fundamentals of absorption and wetting

The contact angle is a quantitative measure of the wetting of a solid by a liquid, providing information about both wetting and spreading. The contact angle is defined geometrically as the angle formed at the intersection of a liquid, solid and gas. The contact angle of a sessile droplet on an ideal solid surface can be described by Young's equation (Eq. 1), which describes

the shape of the drop at the liquid-solid-vapor three-phase contact line under thermodynamic equilibrium:

$$\sigma_{SV} = \sigma_{SL} + \gamma_{LV} \cos \theta_{SL} \quad (1),$$

where θ_{SL} is the contact angle between the solid and the liquid, i.e. the intrinsic contact angle. σ_{SV} and σ_{SL} are the surface energies at the solid-vapor and solid-liquid interfaces, and γ_{LV} is the surface tension at the liquid-vapor interface (De Gennes et al. 2004).

For rough substrates such as paper and paperboard, Wenzel's roughness correction (Eq. 2) can be used if the substrate is hydrophilic ($CA < 90^\circ$) (Wenzel 1936). The equation establishes that the relationship between the measured contact angle (θ_m) and the roughness-corrected angle (θ_c) on an ideal smooth surface may be written as:

$$\cos \theta_m = r \cos \theta_c \quad (2)$$

where r is the topographical correction factor. This factor can be calculated from the S_{dr} roughness parameter, which is the ratio between the interfacial and projected areas and can be measured e.g. with an AFM:

$$r = 1 + (S_{dr}/100) \quad (3)$$

The same approach have also been utilized for e.g. linseed and mineral oils on calcite surfaces (Koivula et al. 2011).

3.2 Liquid penetration into fiber-based substrates

The penetration of a single drop into paper can be described with Bikerman's equation:

$$\frac{d^3}{v} = \frac{(24 \sin^3 \theta)}{(\pi(2 - 3 \cos \theta + \cos^3 \theta))} \quad (4)$$

This equation makes it possible to calculate the volume of unpenetrated liquid v from the drop profile using the contact angle θ and the diameter d of a droplet. The actual volume of penetrated liquid is determined by subtracting the unpenetrated volume at any point in time from the drop's initial volume (Oliver and Forsyth 1990).

Liquid sorption into a fiber-based substrate is commonly described by the Lucas-Washburn equation (Eq. 5):

$$h^2 = \left(\frac{rt}{2\eta}\right) \gamma_{LV} \cos \theta \quad (5)$$

This equation considers the surface as a bundle of parallel capillaries having a certain diameter r and gives the penetration depth h at time t for a liquid with a surface tension γ_{LV} , viscosity η and contact angle θ on the substrate.

However, the Lucas-Washburn equation does not take into account the swelling of the substrate. Bristow (1971) and Bristow (1972) showed that the fibers absorb the water first and swell, after which the pores are filled. The penetration of water into the fibers thus determines the total sorption volume, but the transport of water in the pores is affected by several factors such as vapor diffusion, surface diffusion and water penetration into fibers. For instance, hardwood fibers absorb less water than softwood fibers (Dutt et al. 2012). Therefore, Hoyland (1978) developed a model that includes a correction factor for fiber swelling (Eq. 6):

$$x = \sqrt{\frac{r\gamma_{LV}\cos\theta(t-t_k)}{2\eta}} - K\Delta Z \quad (6)$$

where t_k is wetting delay, K is a constant, and ΔZ is the increase in thickness at time t . This model has some weaknesses (Eklund and Salminen 1987), but it confirms that the swelling of paper affects the liquid sorption.

Particularly in the case of coated papers, the pore size must also be taken into account when the wetting is considered, because the Lucas-Washburn equation is not scalable with respect to pore size (Schoelkopf et al. 2002). A large number of small pores may result in a faster absorption than large pores. This is ascribed to a greater number of possible pathways for the liquid to

penetrate into. The reason for the accelerated absorption is inertial forces that develop soon after the liquid is applied, but this is probably not relevant in the case of barrier materials, although it may affect the setting of aqueous glue layers on pigment-coated substrates (Ninness et al. 2011) or e.g. in printing applications. The short time-scale solution of the Bosanquet equation (Eq. 7):

$$x = t \sqrt{\frac{2\gamma_{LV} \cos \theta}{r\rho}} \quad (7)$$

makes it possible to study the effect of inertia, giving a more realistic image of the wetting-related phenomena on a coated substrate. Liquid viscosity becomes insignificant in inertial flow, but the travelled distance is inversely proportional to the fluid density ρ (Schoelkopf et al. 2000). It has, however, been suggested that the full Bosanquet equation describes the liquid penetration better in the time range $10^{-3} \text{ s} < t < 1 \text{ s}$, and that the short time-scale solution should only be used on an even shorter time scale ($t < 10^{-6} \text{ s}$) (Rosenholm 2015).

Finally, it must be mentioned that complex fluids such as oil-water emulsions may have completely different wetting and absorption properties. Preferential absorption may alter the surface energy of the substrate or one component of the fluid may clog the capillary structure, and both these effects undoubtedly affect the fluid penetration (Rojas 2009). Bearing in mind that the chemical and physical structures of a paper are heterogeneous, it is extremely difficult to describe accurately the wetting-related phenomena with models and an empirical study is often the most informative approach if neither the liquid nor the solid is homogeneous.

3.3 Effect of surface roughness and liquid viscosity

The surface roughness is an important parameter affecting the wetting behavior of oil, since the asperities of a rough surface may retard liquid spreading. Prabhu et al. (2009) studied the wetting kinetics of several different types of oils, including a mineral oil and vegetable oils, on stainless steel surfaces. Oils with a low viscosity spread rapidly, whereas a high viscosity retarded spreading. Furthermore, the time of oil relaxation increased with increasing surface roughness, since the presence of asperities on the surface require a larger driving force if the oil is to be able to spread.

The viscosity of an oil is highly dependent on its temperature (Noureddini et al. 1992; Esteban et al. 2012), and this is an important factor affecting the ability of the oil to penetrate into a material, at least over longer time intervals than the models presented in Chapter 3.2 demonstrate. The oil diffusion rate is smaller if the viscosity is high (Rousu et al. 2002). Khan and Nasef (2009) stated that the wetting kinetics of an oil depend its surface tension and viscosity, but Prabhu et al. (2009) also emphasized the significance of surface roughness. The recorded contact angles of silicone oil and glycerol were higher on rough surfaces at the beginning of the measurement, although the difference in contact angles decreased as time passed by. However, both silicone oil and glycerol are not only rather viscous liquids but also non-volatile compounds, and they are thus not similar to typical probe liquids used for e.g. surface energy determinations. For instance, the results of Kandlikar and Steinke (2002) suggest that an increase in roughness leads to a larger contact angle if the liquid evaporates during the determination.

4 OIL AND GREASE RESISTANCE

The hydrophilicity of cellulose makes it primarily an interesting raw material for use in preventing the penetration of hydrophobic liquids such as oils. The process for manufacturing parchment paper – a high-strength grease-resistant specialty packaging paper – was developed in the 1850s and other types of greaseproof papers have later come onto the market (Gaine 1853). In the manufacture of parchment, a kraft pulp-based web is treated with sulfuric acid that partly dissolves the cellulose and increases the fiber contacts, resulting in a dense paper with excellent wet strength (Twede et al. 2015). The first greaseproof coatings for fiber-based substrates were patented at the beginning of the 20th century. The coatings typically consisted of resin-based solutions (Staples et al. 1899), blends of cassava and wax (Mills 1908) or mixtures of bio-based substances such as blends of gelatin and coconut oil (Wilbur 1923).

The grammage of greaseproof specialty papers is typically low, and the lack of bulk impedes converting thereof. Therefore, surface sizing and coating have become the most widely used methods to produce barrier-grade paperboards. The two basic strategies to affect the oil diffusion into a fiber-based substrate are (i.) the creation of a low energy surface that is thermodynamically capable of repelling the oil or (ii.) the creation of a tortuous physical barrier (Aulin et al. 2008). In addition, the fiber composition affects the oil penetration speed (Dutt et al. 2012).

4.1 Oil repellence – physico-chemical approach

Surfaces with a very low surface energy effectively repel oils. In practice, only treatment with fluorocompounds can provide a sufficiently low surface energy, but the use of these compounds in the creation of oil-repellent surfaces is nowadays limited due to concerns such as poor biodegradability, potential toxicity and accumulation in human tissue (Giesy 2002; Shankar et al. 2001; Yeung et al. 2006). Aulin et al. (2008) found a correlation between the fluorine concentration, the dispersive surface energy and the contact angle of oil on fluorinated cellulosic films. Both coated and covalently modified films were studied. Their findings showed that the dispersive surface energy should be less than 18 mN/m in order to make the film repellent for castor oil. The fluorochemical can also be added to the furnish in the papermaking process (Perng and Wang 2012), but the distribution of the fluorocompound on

the surface of a fiber can be uneven (Brinen and Proverb 1991), and coating is therefore a more effective way of achieving even coverage.

4.2 Oil resistance – physical barrier

Liquid penetration into a substrate can be described by several models (see Chapter 3.2), but modelling the barrier properties of a polymeric coating containing a pigment requires a new approach. Polymer coatings have primarily been used as physical barriers, but most of the coatings are at least slightly permeable due to amorphous regions in the coating, and this limits their applicability for high barrier applications.

The barrier properties of a polymeric coating can thus be improved by e.g. adding a filler or increasing the degree of crystallinity of the polymer film (Hedenqvist and Gedde 1996), both of which increase the proportion of impermeable matrix in the coating. Biopolymer films and coatings are, however, often more permeable, and the utilization of a filler may lead to a substantial increase in barrier properties, probably due to the joint effect of increased tortuosity and the oil absorption capacity of the coating, especially if the mineral is oleophilic (Morabito 2004). At the same time, the penetration of oil into a latex-coated substrate is often a diffusion process, which is slower than capillary absorption (Rousu et al. 2002). This indicates that diffusion-related chemical interactions cannot be neglected and the penetration is highly dependent on the type of latex and its solubility parameter, the oil solubility parameter (aromatic mineral oil > linseed oil > rapeseed oil) and also the molecular size and viscosity of the oil (Rousu et al. 2002).

In the field of dispersion coating, the addition of a high aspect ratio inorganic mineral to a mixture of hydroxypropylated starch and a synthetic polymer has been reported to improve the grease resistance of the coating (Tanninen et al. 2014). Zou et al. (2007) have studied latex-filler systems and found differences between different types of kaolins and calcium carbonates. It has been found that the aspect ratio of the mineral has a significant effect on the barrier properties, including grease resistance, and also that a high oil absorbency of the filler may impair the grease resistance of the coating. However, that suggestion should be questioned, since there is evidence that talc, which is an oleophilic mineral, provides better grease resistance than e.g. kaolin for water-based coatings (Wuu and Rabot 2009). There is also evidence that

the water sensitivity of talc-based coatings is dependent on the presence of water-soluble polymers such as CMC and starch in the recipe (Carne 1997).

4.3 Effect of base substrate on oil penetration

Several factors including the composition of the furnish, the structure of the fiber network and the degree of refining of the pulp affect the greaseproof properties of a fiber-based substrate. Softwood fibers provide higher Kit-values than hardwood fibers, indicating a better grease barrier, although hardwood fibers absorb less water. A correlation between a low Kit-value and high air permeability has been found (Perng and Wang 2012). There is also evidence that blending softwood and hardwood fibers leads to improved greaseproofness. At the same time, it has been shown that fillers in paper are detrimental to the greaseproofness if its grease resistance is based only on a physical barrier, indicating that the use of pigments should be limited to the coating layers. Special attention should be paid to the selection of wet-end additives, since e.g. cationic starch improves the greaseproofness more than ethylated or soluble starches (Perng and Wang 2012). Dutt et al. (2012) have also shown that a minor decrease in the rate of castor oil penetration can be obtained if the stock contains NaHCO_3 , regardless of whether the stock contains hardwood or softwood pulp.

4.4 Effect of fatty acid composition on oil penetration

The blending of vegetable oils has been reported to have certain food-technological benefits instead of using only one oil in the frying process (De Marco et al. 2007). In addition, a recent trend in the food industry has been to replace trans fats with unsaturated fats. Since the most widely used unsaturated fats are not solid at room temperature, packaging materials with better grease resistance are required in order to avoid staining of the package (Twede et al. 2015). Although staining is mainly a cosmetic problem, it is linked to the performance of the packaging material (Lange et al. 2002). Bearing in mind that the food may contain not only the frying oil but also fatty acids originating from the food itself, it is important to study the interactions between the packaging material and different oil blends. Vegetable oils are non-polar or slightly polar compounds, consisting mostly of triglycerides, which are esters of glycerol and fatty acids (O'Brien 1995; Pykönen et al. 2010), and the ratio of saturated to unsaturated fatty acids vary between different vegetable oils. Fatty acids containing double bonds in their alkyl chain are

called unsaturated fatty acids, whereas saturated fats are free from double bonds. The carbon chain of a saturated fatty acid is usually longer than that of an unsaturated fatty acid.

Earlier studies have shown that the penetration time of vegetable oils into a barrier-coated packaging material varies depending on oil type. Both a longer carbon chain length and a greater degree of saturation lead to faster sorption into an extruded polyethylene coating, but there is also evidence that additional double bonds in a certain position of the carbon chain reduce the diffusion rate through a polymer matrix (Olafsson and Hildingsson 1995). Another study that compared the penetration of peanut butter (peanut oil) and canola oil (lower proportion of saturated fatty acids than peanut oil) through a substrate with a UV-cured coating suggested that canola oil penetrates faster than peanut oil (Ramsey 2012). This finding not only illustrates the difference in diffusion of different types of oils, but also emphasizes the role of the coating. Furthermore, the penetration of a fat blend differs from that of a single-component fat. For instance, a mixture of pork and poultry fat penetrates faster through a polyethylene-coated paperboard than pure poultry fat (Lange et al. 2002).

5 OIL AND GREASE BARRIER PROPERTIES OF CONVERTED PAPERS AND BOARDS

Hybrid printing, where digital printing methods are used together with conventional methods for printing customized information and creating small details in packages, is of great interest (Viström 2008). At the same time, adhesion problems between a film and a fiber-based substrate are often reduced by modifying the surface energy levels by corona or plasma treatment. These treatments may increase the number of corona exposures to which the substrate is exposed during its manufacturing and finishing processes. Since corona discharge modifies the surface properties, which in turn alters the wetting-related phenomena, there is obviously a need to discuss the effects of corona treatment on barrier properties of packaging materials. Furthermore, the effects of mechanical converting on barrier properties should be taken into account when discussing the oil and grease resistance of packaging materials.

5.1 Fundamentals of surface treatment of fiber-based substrates with corona

Corona treatment is a common way of pretreating paper and paperboard products to modify the surface of the substrate by high energy ions such as O^- , CO_3^- , O_3^- created by a negative discharge (Shahin 1969) and HO_2^+ , N_2H^+ and $(H_3O)^+ \cdot (H_2O)_n$ created by a positive discharge (Shahin 1966). The high-polarity species affect the surface energy, which leads to several benefits such as improved heat-sealing properties of packaging materials, better adhesion of a polymer film onto a paperboard and enhanced printability of the substrate by decreasing ink spreading and improving ink adhesion (Lahti and Tuominen 2007; Mesic et al. 2005; Vyörykkä et al. 2011).

Corona treatment has been reported to increase the roughness of pigment-coated papers (Pykönen 2010), but plastic films behave differently. The change can be only very small or the film may even become smoother (Földes et al. 2000; Strobel et al. 2003). A rougher surface retards or reduces the spreading of oils, since a greater driving force is required for the liquid to be able to overcome the surface asperities (Khan and Nasef 2009; Prabhu et al. 2009). As stated in Chapter 3.3, roughness is one factor that affects the wetting kinetics, but it must be remembered that the mechanism preventing the diffusion of liquid is based on a physical barrier in the case of polymeric films, and hence the barrier properties cannot be judged merely from the liquid-spreading kinetics.

The chemical compositions of the substrate and its coatings have a substantial influence on corona-induced charging and polarization behavior. Although cellulose is the component that determines the polarizability of a paper-based substrate (Sidaravicius et al. 2013), the effect of other substances in the paper or paperboard on the polarization cannot be ignored. The dielectric constant and dielectric losses define the polarizability of a material and strong polarization takes place if the conductivity is high due to the presence of ions. Furthermore, the relative humidity has a significant effect on the dielectric properties of a coated paper (Simula et al. 1999, Backfolk et al. 2010). The oxidation potential of a material depends on the amount of hydroxyl groups (-OH). The oxidation of certain fillers such as talc is thus difficult due to a small number of -OH groups, but biopolymers such as cellulose have a high number of -OH groups, and this assists polarization. However, the matter is not completely black-and-white, since there are differences between inorganic minerals. The polarizability of talc in paper has been reported to be lower than that of kaolin clay, that contains more -OH groups than talc, or calcium carbonate (Sidaravicius et al. 2013), which confirms the inert nature of talc and indicates that it is a less electrically conductive mineral. The polarizability of inorganic minerals is substantially lower than that of synthetic latices (Pykönen 2010).

Coated papers generally have a higher charge acceptance than uncoated grades, and there is a material-dependent limiting value for the charging potential, above which the charging potential does not increase further with increasing corona voltage (Sirviö et al. 2009). Since the fiber-based bulk matrix has a lower electrical conductivity than a pigment coating, it can be assumed that an increase in the electrical conductivity of the coating layer decreases the overall charging capability of a corona discharge (Backfolk et al. 2010). From the viewpoint of a dispersion coating containing a pigment, this may suggest that an increase in the proportion of pigment in the coating layer will decrease the degree of bulk treatment, leading to greater changes in the coating layer.

5.2 Over-treatment and reverse-side effects

A typical challenge in corona treatment is to achieve the desired treatment level without harming the usability of the substrate. Over-treatment may cause e.g. surface delamination, problems in ink-substrate interactions and poorer heat-sealability, and this means that the treatment level should be optimized separately for each substrate. In addition, an increase in the intensity of reverse-side effects (sometimes also referred to backside treatment) can also be

seen (Wolf 2007). The origin of the reverse-side effects is shown in Figure 5.1, where the air trapped between the backing roll and the reverse side of the substrate becomes ionized due to either corona strike through or substrate porosity, leading to the passage of the corona discharge to the reverse side (Cernakova et al. 2006; Väänänen et al. 2010). Rough or wrinkled substrates are particularly problematic (Wolf 2007).

The amount of applied energy remains constant whether or not reverse-side effects occur, and hence there will be a reduction in the treatment level on the top side while the reverse side becomes treated. If the reverse side also becomes treated, it is reasonable to expect that the blocking and picking tendency of the material may increase (Wolf 2007; Lindell et al. 2011), the first of which is controllable by adding a mineral filler to the top coating (Kugge and Johnson 2008).

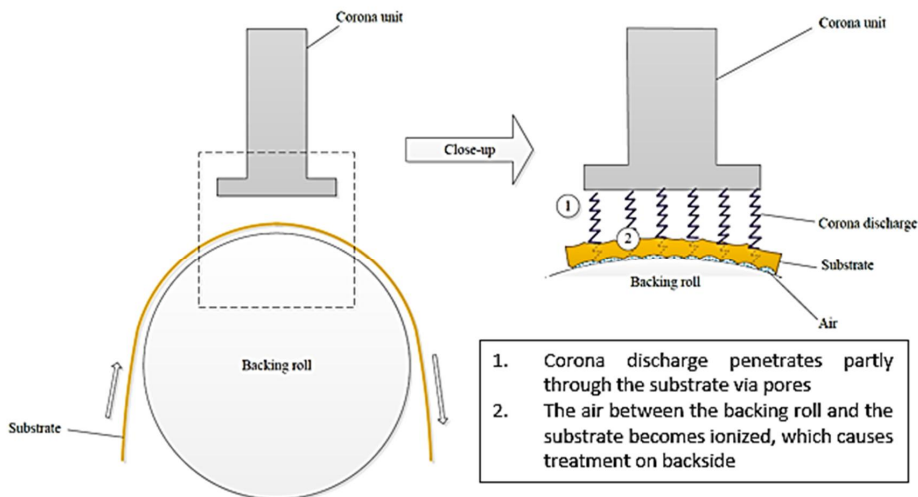


Figure 5.1 The mechanism of reverse-side corona treatment on a rough, porous substrate.

5.3 Effect of corona treatment on barrier properties

The effect of the intensity of corona treatment on the barrier properties of a substrate is an important topic for several reasons. Surface charging and polarization increase with increasing treatment level, but simultaneously the prevalence of strike through increases (Cernakova et al. 2006) and the fibers may even become damaged by pinholing (Vander Vielen and Ragauskas 2002). Strike through occurs when the voltage of the corona discharge is sufficiently high to

change the electrical conductivity of the substrate or of a part of it, leading to rapid gas or liquid penetration. Despite of potential harmfulness of corona treatment to barrier properties, only a limited number of studies of this topic have been reported. Schumann et al. (2005a) observed that the intense corona treatment of a latex-based dispersion coating resulted in an increase in WVTR, indicating a loss of barrier properties. Plasma treatment did not impair the water vapor barrier. The results of Hirvikorpi et al. (2010) nevertheless question the detrimental effect of a corona discharge. In fact, it was shown that the WVTR of extrusion-coated boards might even decrease after the substrate had been corona treated, which suggests that corona can induce self-healing. Both these findings emphasize that the power level must be optimized for each substrate separately, and suggest that there are coating-related particularities that define the corona-induced alterations in barrier properties. Together with the coating composition, the thickness of the coating layer is an important parameter that affects its sensitivity to corona treatment (Bollström et al. 2011).

In addition to surface-related changes, alterations in internal wetting may occur. This problem is emphasized with porous substrates and is linked to the reverse side effects, discussed in Chapter 5.2. Internal treatment occurs when the ions that arise from the corona treatment penetrate into the porous matrix. Furthermore, a secondary corona discharge can take place in the pores, and this may affect the liquid penetration (Galanti et al. 2012; Väänänen et al. 2010).

Finally, there is a particularly interesting feature in the interaction between oils and corona-treated surfaces. Pykönen et al. (2010) studied offset ink components and showed that the contact angle of mineral oil (hydrocarbons) on a pigment-coated paper remains unchanged after corona treatment, but a minor decrease in the contact angle of linseed oil (ester) was detected. This finding suggests that it is important to study the vegetable oil wetting behavior as a function of time on corona-treated packaging materials in detail, since there seem to be differences in wetting kinetics.

5.4 Effects of mechanical converting on the barrier properties of biopolymer-coated paperboards

The tendency of biopolymer coatings to crack under mechanical forces is often quite high compared to that of plastic extrusion coatings. In press-forming process, the cracks mostly occur in the corner areas of produced trays due to the geometry, and the occurrence of cracks

is highly dependent on the mould temperature (Tanninen et al. 2014). Tanninen et al. (2015) studied the creasability of HPS-based dispersion coatings by evaluating the microcracks with microscopic methods, and they found that the creasing force must be 30% lower than with extrusion coatings in order to obtain the required quality of the creases. Both die-cutting and creasing processes also led to pinholes in the bio-based coatings, and this destroyed the grease-barrier properties of the materials. On the other hand, selecting a straight creasing groove instead of a conical one and avoiding the use of worn grooves decreased the prevalence of pinholes. Similar results with HPS have also been published by Annushko (2013), who found that a high content of gelatin moderately compensates for the negative effect of creasing on grease resistance. Gogoleva (2013) studied the grease resistance of creased paperboards with cellulose-derivative-based coatings, and found that the creased area has no ability to resist grease. Machine-directional creases damaged the coating severely, but faster grease penetration was also recorded on cross-directional creases. In the region where a machine-directional and a cross-directional crease cross each other, the grease penetration time was similar to that of a machine-directional crease.

EXPERIMENTAL

6 MATERIALS AND METHODS

The experimental methods and materials used in the work described in this thesis are summarized in this chapter. More detailed descriptions are given in Papers I–VI. The generalized targets, the research questions and the compositions of the studied coatings are presented in Table 6.1.

Table 6.1 The experimental design of the studies presented in Papers I–VI.

	Paper I	Paper II	Paper III	Paper IV	Paper V	Paper VI
Target	To clarify the heat-induced effects in dispersion coatings	To study grease penetration with blended oils	Presentation of a novel and easily controllable lab-method for CT ¹	To clarify the corona-induced alterations in dispersion coatings	To study the occurrence of reverse side effects and their influence on OGR ²	To study the effects of press forming on OGR ²
Research question	How does heat exposure alter the OGR ² ?	Differences in the penetration of fatty acids?	Applicability of modified BAA ³	Does corona treatment impair the OGR ² ?	Do reverse side effects impair the OGR ² ?	How does converting affect the OGR ² ?
Barrier dispersion	HPS SB-latex Talc	HPS SB-latex Talc	(a)	HPS SB-latex Talc	HPS SB-latex Talc	HPC SB-latex Talc Gelatin
Pre-coating ^(b)	-	-	-	-	-	CMC Gelatin MFC
Number of coating layers	Double-coated	Double-coated	(a)	Double-coated	Double-coated	Double-coated (+pre-coating)

¹ CT – corona treatment

² OGR – oil and grease resistance

³ BAA – Bristow absorption apparatus

(a) The applicability of the method was confirmed by testing multi-layered polyelectrolyte coatings designed for printing purposes

(b) The addition of a pre-coating layer with one barrier dispersion was studied in order to maximize convertability in a press-forming process

6.1 Coating process and substrate

In Papers I–II and IV–V, the smoother side (Bendtsen roughness was 880 ml/min; rougher side had a roughness of 1140 ml/min) of SBS paperboard sheets (Trayforma Natura, Stora Enso Oyj, Imatra, Finland) with a grammage of 350 g/m² were double-coated with a regular bent-

blade in a pilot coater (DT Paper Sciences, Finland) at a speed of 10 m/min. The targeted coat weight was 8 g/m² (4 g/m²/layer). Coated samples were dried with an infrared dryer with a heating power of 6 kW. The distance between the dryer and the coated substrate was approx. 8 cm. The drying time was 9–12 seconds, depending on the proportion of pigment in the coating dispersion. In Paper VI, the same paperboard was double-coated in a web mode with a carbide-tipped bent-blade. The targeted coat weight was 5 g/m²/layer. An additional infrared-dryer (2 kW) was positioned after an air dryer in order to increase the drying capacity. The effect of an additional pre-coating layer (2 g/m²) was also studied in Paper VI.

6.2 Coating dispersions

In Papers I–II and IV–V, dispersion barrier coatings containing pigments were prepared using barrier-grade talc (Finntalc C15B, Mondo Minerals B. V., Finland) with a mean aspect ratio of 0.6 and an average particle size of 11 µm (bimodal particle size distribution), low-viscous potato-based hydroxypropylated starch (Solcoat P55, Solam GmbH, Germany) and styrene-butadiene latex (SB₁; Styron HPW-184, Styron Europe GmbH). The glass transition temperature of the latex was -9°C, and the mean particle size was 160 nm. The dispersions contained 0–30 pph of talc and 0–10 pph of latex. The latex amount was calculated in relation to the total dry mass of the other components, talc and starch. All the dispersions were prepared using a Diaf mixer (Pilvad Diaf, Denmark), and the dry solids content was adjusted to 16.5 wt% with tap water. The dispersions used in Paper VI were prepared in the same way, but the hydroxypropylated starch was replaced with hydroxypropyl cellulose (Klucel J-Ind, Ashland), the SB-latex used was Styronal D517 (SB₂; BASF GmbH), and the dry solids content of the dispersion was 12%. In addition, 0–5 pph of gelatin (Meira, Finland) was added to the dispersion in order to reduce the brittleness of the coating layer. The effect of a CMC-based (Finnfix 30, CP Kelco Oy, Finland) pre-coating layer (2 g/m²) was also studied. The dispersion recipes are shown in Table 6.2.

Table 6.2 Barrier dispersion recipes.

	Biopolymer	Synthetic polymer	Pigment
Paper I	HPS (70-100 pph)	SB ₁ (0-10 pph)	Talc (0-30 pph)
Paper II	HPS (70-100 pph)	SB ₁ (0-10 pph)	Talc (0-30 pph)
Paper III	<i>Dispersion coating was not studied</i>		
Paper IV	HPS (70-100 pph)	SB ₁ (0-10 pph)	Talc (0-30 pph)
Paper V	HPS (70-100 pph)	SB ₁ (0-10 pph)	Talc (0-30 pph)
Paper VI	HPC (70-100 pph)	SB ₂ (0-10 pph)	Talc (0-30 pph)

6.3 Corona treatment and chemical composition of coated surfaces

6.3.1 Design of the corona treatment apparatus

The objective of Paper III was to develop a laboratory-scale apparatus for treating substrates with corona *in a controllable manner* and to apply ink at velocities relevant to desktop printing. A Bristow Absorption Apparatus was equipped with a corona charger as shown in Figure 6.1. The unit allows both direct current and alternating current (plasma) treatments, although only direct current corona was used in this work. In Papers IV–V, direct current corona was used with positive and negative voltage polarities. The treatment was carried out in a manner similar to the regular Bristow method (Bristow 1967), except that no test liquid was used in the experiments in Papers IV–V. The treatment level, which depends on the corona voltage, distance and wheel rotation rate, was evaluated as the corona current energy flow through the paper in $W \cdot \text{min}/\text{m}^2$, and ranged from -400 to $+400 W \cdot \text{min}/\text{m}^2$. Both coated and uncoated sides were treated. Unusually high treatment levels were chosen, since preliminary trials showed only a very minor effect on surface energy with a treatment efficiency typical of industrial converting processes (approx. $50 W \cdot \text{min}/\text{m}^2$, Tuominen et al. 2010).

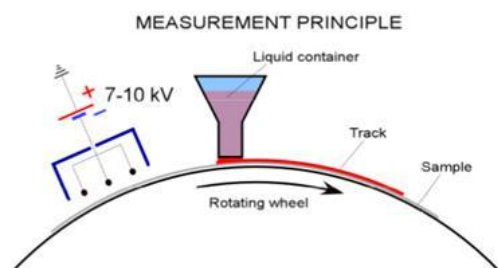


Figure 6.1 Schematic illustration of measurement principle using the modified Bristow wheel. Reprinted with permission of IS&T: The Society for Imaging Science and Technology sole copyright owners of NIP30: International Conference on Digital Printing Technologies and Digital Fabrication 2014.

6.3.2 Chemical analysis of the surfaces

In order to study the effects of heat treatment (two minutes at 100°C ; for details, see Paper I) and corona treatment (for details, see Papers IV–V) on the chemical composition of the surfaces, the samples were analyzed using X-ray photoelectron spectroscopy (XPS, Axis ULTRA, Kratos Analytical) with low-power monochromated Al $K\alpha$ irradiation (at 100W)

under neutralization. Low-resolution survey scans (80 eV pass energy, 1 eV step) were used to determine the elemental surface composition, and high-resolution C 1s regions were recorded to obtain more detailed chemical information, especially with regard to the carbon compounds observed. The area of analysis was 400 μm x 800 μm and each sample was analyzed at 3–5 locations.

6.4 Preparation of oil blends and their characterization

The objective of Paper II was to clarify the effect of oil fatty acid composition on the penetration of the oil into dispersion-coated boards using mixtures of saturated (coconut oil) and unsaturated (rapeseed oil) oils. Both rapeseed and coconut oil were preheated in an oven at 60°C before being carefully mixed. To avoid solidification of the coconut oil, the oil mixtures were stored at 60°C. The compositions of the oil mixtures are shown in Table 6.3.

Table 6.3 Ratios of saturated and unsaturated fats in coconut and rapeseed oil, and the compositions (pph) of the oil blends.

	Oil No.					
	1	2	3	4	5	6
Coconut oil, [pph]	0.0	14.6	38.4	62.2	86.0	100.0
Rapeseed oil, [pph]	100.0	85.4	61.5	37.8	14.0	0.0
Saturated fat, [pph]	7.5	20	40	60	80	91.8
Unsaturated fat, [pph]	92.5	80	60	40	20	8.2

The surface tensions of the oils were determined with a Theta optical tensiometer (Biolin Scientific AB) at 25°C using a needle with a gauge of 30, the drop size being 6.70 μl , and an average value of five independent measurements was reported. The dynamic viscosities of the vegetable oil blends were measured with a Rheometer (Anton Paar Modular Compact Rheometer, MCR 302). In the measurements, a standardized double gap DG 26.7/T200 measurement cylinder was used. The viscosities were measured using shear rates in the range of 10–1000 s^{-1} the temperature being 60°C, which was the same as the ambient temperature in the grease resistance determinations.

6.5 Contact angle and surface free energy determinations

Apparent contact angles were determined with a Theta optical tensiometer (Biolin Scientific AB) using deionised water, 99.8% ethylene glycol (EG, VWR S.A.S. International, France),

99% diiodomethane (DIM, Alfa-Aesar GmbH & Co KG, Germany) and rapeseed oil (Bunge Finland Oy) as test liquids. The droplet volumes were 3 μl for deionised water and EG, 1 μl for DIM, and 5 μl for rapeseed oil. A needle of 22 gauge was used for all the liquids except the rapeseed oil, which was dispensed with a 30-gauge needle. A 420 Hz camera (Basler A602F-2 with Navitar optics) was used to capture images of the drop dispensed on the substrate. Digital images were analyzed with the OneAttension image tool. The baseline was set manually in all cases. The surface energies were calculated from the contact angle data of DIM, EG, and water using the Lewis acid-base approach. The average values of three independent measurements were reported.

6.6 Imaging methods

6.6.1 Coating coverage and study of sealing surfaces

Scanning electron microscopy (SEM) was used to study coating coverage and the possible occurrence of pinholes or blisters in the coatings. In Paper I, SEM images were taken using the composition mode (COMPO) at an acceleration voltage of 10 kV with a working distance of 10.7–14 mm. In Paper VI, the surfaces of the samples were imaged with a Jeiotech JEOLJSM-5800 SEM using a secondary SEI-detector with an acceleration voltage of 15 kV. In addition, the sealing surfaces of the trays (for details, see Leminen et al. 2015) were investigated with a stereomicroscope in order to compare the creases on the commercial PET-coated reference sample with those on the experimental paperboard.

The smoothness of the coated surface was also evaluated with an optical profilometer (Rodestock RM-600-S) in accordance with ISO 25178.

6.6.2 Physico-chemical analyses with an atomic force microscope

In Paper I, atomic force microscopy (AFM) measurements were made in the PeakForce QNM scanning probe mode (Bruker Multimode 8, Bruker Corp.). The samples were tested in-situ before, during and after heat treatment at 95°C. Stiff probes with a spring constant of 42 N/m and a tip radius of 10 nm were used. The sample was heated in 1.5°C steps with a temperature equilibration time of 5 min. The measurement area was 8 x 8 μm and topography, DMT modulus, and adhesion images were taken. In Paper IV, the Sneddon modulus was also

investigated under ambient conditions ($25 \pm 3^\circ\text{C}$; $40 \pm 10\%$ RH). The roughness parameters used for correcting the contact angles were calculated from three independent measurements.

6.6.3 Oil penetration studies with a confocal laser scanning microscope

The objective of Paper II was to study the differences in penetration between saturated and unsaturated fatty acids. Confocal laser scanning microscope (CLSM, Leica TCS SP5 AOBS, Germany) images were used to characterize the microstructure of the coated paperboards and to study the oil penetration as a function of time (imaging interval 10 s). A PL APO objective with a magnification of 10x and a numerical aperture of 0.40 was used throughout the study. The light source was an argon laser with an emission maximum at 488 nm. The emitted signals were recorded in the wavelength interval of 500–650 nm. The microstructure of the coated samples was recorded by utilizing the autofluorescent signal of the fibers. The oil penetration was made visible by mixing 200 ppm fatty acid BODIPY FL C16 (Invitrogen Molecular Probes, Eugene, Oregon, USA), into the rapeseed and coconut oils.

In the measurement, a 10 mm wide sample was attached to a cover glass slide with an adhesive so that the cross-section of the coated paperboard was facing the objective. Oil was added to one side of the coated paperboard, which made it possible to record the oil penetration through the coated sample. Fluorescence recovery after photobleaching (FRAP) measurements were carried out and analyzed as described elsewhere (Schuster et al. 2014). The imaging allowed the determination of the mass transport (diffusion coefficients for oils) at high spatial resolution.

6.7 Oil and grease resistance

In Papers I–II and IV–VI, the oil and grease resistance were determined using dyed palm kernel oil in accordance with ISO 16532–1 at 60°C . The volume of pipetted oil was approx. 200 μl and only the coated sides of the samples were tested. In order to investigate how temperature affects the grease resistance, the test was carried out at both room temperature ($23 \pm 1^\circ\text{C}$) and an elevated temperature (100°C) (Paper I). The chosen temperatures simulated dry food storage at room temperature and end-use applications in which the packaging material is used for serving hot food or as a tray in a microwave oven. In Paper II, the determination was carried out at 60°C using the oil mixtures presented in Table 6.3.

In Paper VI, the effect of the press-forming process on the barrier properties was investigated by determining the oil resistance at the tray corners at 60°C (Figure 6.2). The corner area was considered the most demanding region in the tray from the viewpoint of grease barrier due to its curved shape and large number of creases. In the experiment, the tray was positioned at an angle of 45°, and 200 µl of dyed palm kernel oil was injected into the corner. The shape of the area to be measured prevented the use of the standard weight. Additional data of the oil and grease resistance on manually creased areas (convergence of machine- and cross-directional creases, made by a Fastbind C400 creaser, Fastbind International, Finland) is reported in Chapter 7.4.1.



Figure 6.2 Positioning of trays in OGR testing (left) and a close-up of an oil stain at a tray corner.

7 RESULTS AND DISCUSSION

7.1 Oil and grease resistance of non-converted boards (Papers I-II)

The roles of viscosity and fatty acid composition on the penetration time of oils were studied in accordance with ISO 16532-1 at different temperatures using substrates with HPS-based coatings. The measurement was carried out using palm kernel oil dyed with Sudan red, rapeseed oil and coconut oil. Palm kernel oil and coconut oil consist mainly of saturated fatty acids, whereas the fatty acids present in rapeseed oil are mostly unsaturated. In addition, the diffusion characteristics of rapeseed and coconut oils were compared by CLSM imaging.

7.1.1 Effect of ambient temperature on oil penetration time

Table 7.1 shows the penetration times of dyed palm kernel oil through the hydroxypropylated-starch-based samples. The OGR was highly dependent on both the temperature and the proportion of talc in the coating. The combination of HPS and SB-latex without talc did not provide an appreciable oil barrier, but the presence of latex improved the grease barrier if talc was present, particularly at room temperature. At higher temperatures, the difference between latex-containing and latex-free coatings was smaller, which was ascribed to the melting of the latex. The positive effect of adding a small amount of synthetic polymer to a dispersion coating has earlier been found by Tanninen et al. (2014), who showed that the convertability and barrier properties (Kit-test) of HPS-based composite coatings could be improved by adding a polyolefin.

At 100°C, the oil penetration time was drastically shortened in all cases, which suggests that the use of HPS-coatings at high temperatures in food-related applications is limited. Together with a decrease in oil viscosity, the poor thermal stability of dual-polymer dispersion coatings (see Chapter 7.3.1) seems to be a factor leading to a poorer oil and grease barrier at high temperatures. However, the heat-induced movement of the coating components does not explain why the OGR values of a *pure HPS coating* are also lower at higher temperatures. This implies either that the diffusion characteristics depend on the viscosity of the oil or that the increase in temperature affects both the oil viscosity and the structure of the coating. The moisture content of mostly bio-based coatings is probably relatively high, and the evaporation

of bound water may create channels in the coating layer, along which the oil can easily penetrate.

Table 7.1 Penetration time of dyed palm kernel oil at 23°C, 60°C and 100°C through samples with HPS-based coatings. S denotes starch, T talc and L latex.

Coating	Penetration time, [min]					
	t _{23°C}	s.d. _{23°C}	t _{60°C}	s.d. _{60°C}	t _{100°C}	s.d. _{100°C}
S100	210	±42	180	±0	1	±0
S100:L10	15	±0	3	±1	1	±0
S85:T15	210	±42	45	±26	3	±1
S85:T15:L10	240	±0	200	±69	23	±11
S70:T30	60 h	±0	>24 h	±0	210	±42
S70:T30:L10	>120 h	±0	>24 h	±0	270	±42

Figure 7.1 shows that the OGR was highly dependent on the oil viscosity. The viscosity of palm kernel oil at different temperatures has earlier been reported by Latinwo et al. (2010), and their results were utilized in this comparison. At room temperature, the viscosity of palm kernel oil was approx. 105 mPas, but at 100°C, it was only approx. 10 mPas. The samples with 30 pph of talc showed a particularly good linear correlation between OGR and viscosity, but in the cases of S100 and S85:T15:L10 coatings, the correlation was weaker compared to other materials. It thus seems that the correlation is greater if the initial grease resistance is good and the proportion of talc of the coating is high, which suggests that the reduced solubility of the coating layer may also assist the coating in resist the oil penetration.

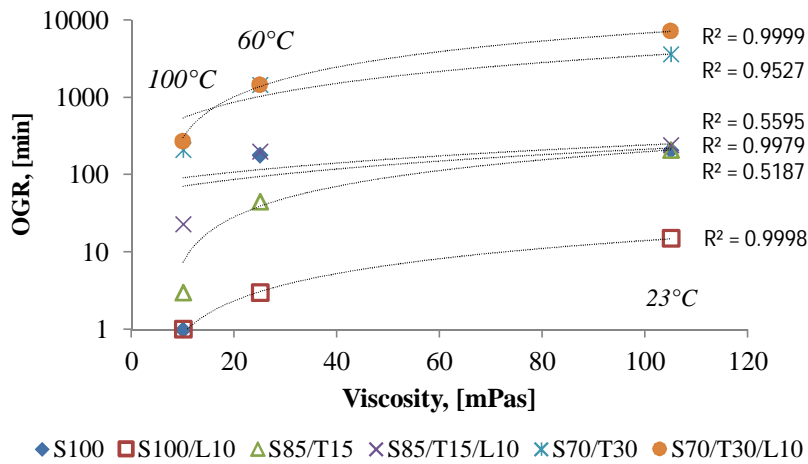


Figure 7.1 Oil and grease resistance of HPS-based coatings as a function of palm kernel oil viscosity. Note logarithmic scale on y-axis.

To investigate the differences between different types of edible oils and their blends, dynamic viscosities of rapeseed and coconut oils were determined at 60°C in the shear rate range 10–1000 s⁻¹. Figure 7.2 shows the viscosities of the oils as a function of saturated fatty acid content with a shear rate of 100 s⁻¹. Pure rapeseed oil had a slightly higher viscosity than coconut oil but the shear rate affected the viscosity only a little. The viscosity of the rapeseed oil at a shear rate of 100 s⁻¹ was 16.4 mPas and that of coconut oil was 13.2 mPas. The measured value for coconut oil agrees well with previous results (13.3 mPas; Nouredini et al. 1992), but the viscosity of rapeseed oil differed from the previously reported value (21.4 mPas; Nouredini et al. 1992). However, the viscosity of rapeseed oil agrees well with the work of Esteban et al. (2012) if their reported kinematic viscosity value is transformed to dynamic viscosity (16.6 mPas). As expected, the viscosity of the oil blends decreased when the proportion of coconut oil was increased.

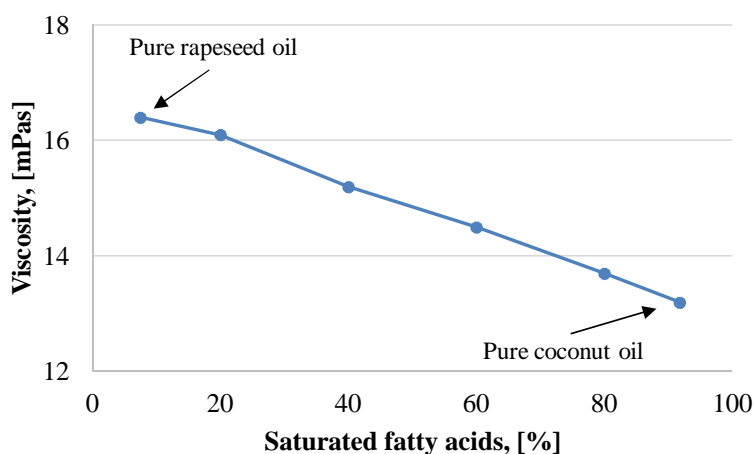


Figure 7.2 Effect of oil composition on the viscosity (shear rate 100 s⁻¹, temperature 60°C) of the oil.

7.1.2 Effect of oil fatty acid composition on oil penetration time and behavior

The penetration time of the oil blends was highly dependent on the pigmentation level (0–30 pph) of the coating and on the proportion of saturated fatty acids in the oil (Figure 7.3). The penetration time of rapeseed oil and oil blends with an unsaturated fatty acid content of 40–80 pph increased with increasing talc content, whereas oils with high content of saturated fatty acids behaved differently. Pure rapeseed oil penetrated more slowly than the coconut oil through the coating with a talc proportion of 30 pph, which was attributed to a preferential oil

absorption mechanism, possibly due to the smaller molecular size of coconut oil. The results of the samples *with 30 pph of talc* agree well with the earlier literature, since (i.) the penetration of mostly saturated coconut oil was faster than that of mostly unsaturated rapeseed oil (Olafsson and Hildingsson 1995), (ii.) the oil heterogeneity increased the penetration time (Ovaska and Backfolk 2013), and (iii.) an increase in the degree of unsaturation resulted in slower penetration (Olafsson and Hildingsson 1995).

The earlier literature does not, however, explain why the oil blends penetrated faster than pure oils with pigmentations of 0–20 pph, although similar results have been reported by Lange et al. (2002). A comparison between OGR and oil viscosity with talc contents of 0–20 pph did not reveal obvious trends, although with 30 pph of talc a correlation can be seen (Figure 7.2). This finding was attributed to a joint effect of

- high content of oleophilic matter, i.e. talc,
- faster penetration capability of saturated fatty acids due to smaller molecule size, which may also affect the oil-binding capacity of talc and starch, and
- higher grease resistance of the material with 30 pph of talc compared to other coatings.

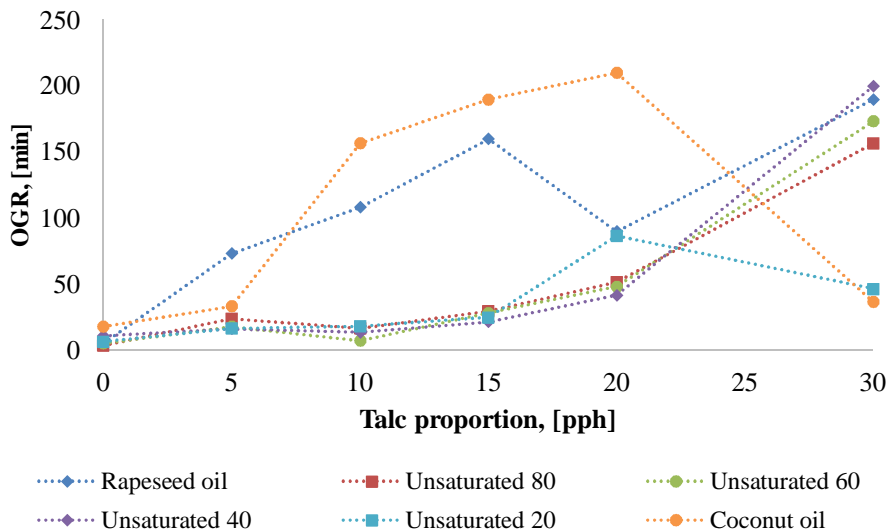


Figure 7.3 Penetration times of rapeseed oil, coconut oil and their blends as a function of the proportion of talc in the coating. The temperature was 60°C.

7.1.3 Cross-sectional analysis of oil diffusion into dispersion-coated board

The penetration of coconut and rapeseed oils into the substrate with a S70:T30:L10 coating was investigated with a CLSM. Figure 7.4 shows the cross-section images of paperboard after penetration of coconut oil and rapeseed oil. Since the imaging was conducted at room temperature, crystallization of coconut oil was expected, and the crystals formed are clearly visible in Figure 7.4A. Interestingly, coconut oil also crystallized inside the coating layer, not only on the coated surface. Crystallized oil was not detected inside the substrate. Bearing in mind that the food industry is striving to replace saturated fats with unsaturated fats, this finding may also have some practical importance. For instance, the melting and crystallization behavior of lard can be adjusted by the addition of rapeseed oil (Cheong et al. 2009). The accumulation of coconut oil inside the coating layer may also explain why the grease penetration times were shorter with highly saturated fats than with mostly unsaturated oil blends (Figure 7.3), since it might be possible that accumulated oil induces swelling of the coating layer. The swollen coating layer may increase the solubility of oil-based components in the coating, resulting in a loss of food aroma (Hernandez-Muñoz et al. 1999). Since this phenomenon was only observed with coatings containing 30 pph of talc, it seems that the component responsible for oil accumulation is the oleophilic talc. In turn, this leads to the conclusion that the ability of talc to bind rapeseed oil is poorer, maybe because of differences in molecular size. In addition, it must be remembered that other components present in food may also affect the crystallization behavior of vegetable fats (Svanberg et al. 2011), which emphasizes the importance of studying the diffusion behavior of different types of oils.

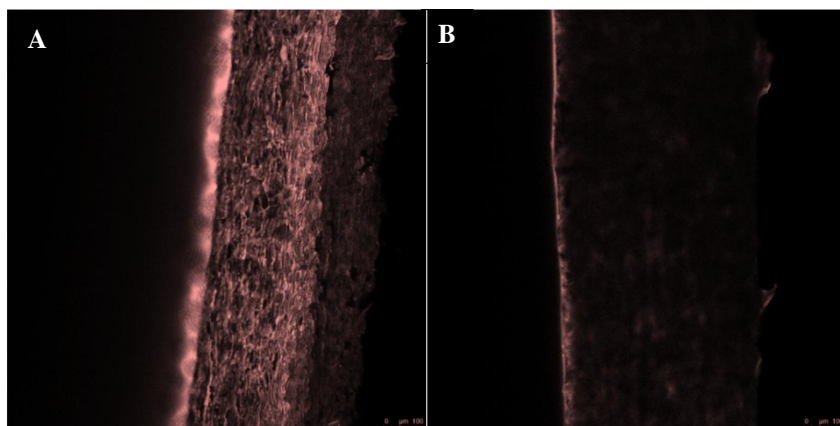


Figure 7.4 Cross-sectional CLSM images of A) coconut oil on board surface and B) rapeseed oil on board surface.

Since the crystallization of coconut oil probably had an effect on the oil diffusion characteristics, only rapeseed oil was chosen for further inspection. The same coating, S70:T30:L10, was again used. Figure 7.5 illustrates the penetration of rapeseed oil in the time range of 0–40 min. The stained oil reached the middle region of the coating already after approx. two minutes. In addition, the fluorescence of the fiber matrix increased throughout the test period, which made it possible to follow the oil penetration. However, all the oil did not penetrate through the coated sample since (i.) starch has a tendency to bind oil to a certain extent (Seguchi 1984) and (ii.) talc is an oleophilic mineral. The ability of the coating to absorb the oil can be seen as an increase in the intensity of the red color of the coating layer (cf. 0 s and 40 min).

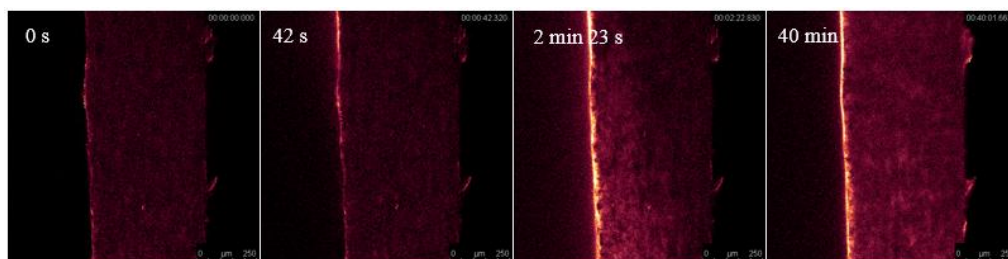


Figure 7.5 Cross-sectional CLSM images illustrating the penetration of rapeseed oil at different points in time. The oil was placed on the coated side of the sample.

To clarify the differences in diffusion characteristics of rapeseed and coconut oils, their diffusion coefficients were determined by exploiting the FRAP mode of CLSM. The results are shown in Figure 7.6. In general, minor differences in the diffusion of coconut and rapeseed oil were revealed, particularly in the bulk matrix (paperboard). The first region of interest (position 1) was located in the middle of the coating layer, relatively close to the outer surface. The second position was in the region close to the coating-paperboard interface. The diffusion coefficient of stained rapeseed oil at these regions was slightly higher than that of coconut oil, although all the differences were within the standard deviations. The third position was the middle region of the paperboard substrate. In this bulk region, the diffusion of rapeseed oil was faster, indicating that the fiber matrix let the rapeseed oil penetrate more rapidly than the coconut oil, which was ascribed to the tendency of coconut oil to solidify at low ambient temperature, 23°C. No major differences in the diffusion were observed in the fourth region, located close to the reverse side of the paperboard.

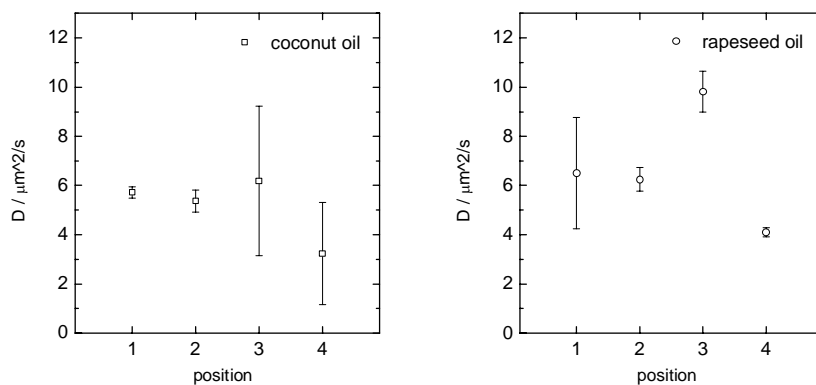


Figure 7.6 Diffusion coefficients at different positions in the board of coconut oil (left) and rapeseed oil obtained with the FRAP mode of CLSM for dispersion-coated board with 30 pph of talc in the coating.

7.2 Effect of electrical treatment on oil-substrate interactions (Papers III-V)

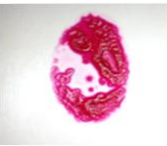
The aim of this chapter is to present the effects of direct-current corona treatment on HPS-based barrier coatings. In Paper III, a controllable laboratory-scale apparatus for corona treatment was developed (see Chapter 6.3.1). In Paper IV, the oil-substrate interactions were studied with contact angle and OGR determinations. Chemical alterations induced by the polarity of the corona discharge were studied with XPS and surface free energy determinations. Physical changes in the coatings as a result of the corona treatment were investigated by imaging the coated surfaces with AFM before and after corona treatment. Paper V deals with the reverse-side effects of corona discharge (sometimes also referred to as backside treatment). In all cases, the differences between a positive and a negative voltage polarity were discussed. Finally, the findings are summarized to evaluate the suitability of the experimental barrier coatings developed for corona-based finishing and converting processes.

7.2.1 Corona-treated dispersion barrier coatings

Before discussing oil-substrate interactions on corona-treated HPS-based coatings, it is useful to consider the behavior of oils on untreated surfaces. Selected key figures are presented in Table 7.2. Firstly, it can be seen that the experimental coatings provided good grease resistance, although the coat weight was significantly less than that of commercial PET-coated sample. On the other hand, an increase in the proportion of talc in the coating and the introduction of latex

improved the OGR of the coated board. The contact angle of water was smaller on all the coatings than on the uncoated surface. A high proportion of HPS increased the hydrophilicity of the surface, illustrating well the common problem related to the water-sensitivity of bio-based coatings. However, the difference between the PET coating and the experimental S70:T30:L10 coating was small, suggesting that latex and talc can both be used to reduce the water-sensitivity of the HPS-based coatings. All the substrates were oleophilic; the contact angle of rapeseed oil increased only slightly regardless of the coating. The coatings had a lower surface free energy (SFE) than the uncoated board. A simple test of the appearance of an oil drop on the substrate after 24 hours revealed significant differences in oil behavior on these surfaces: the uncoated sample absorbed the dyed palm kernel oil completely, whereas uniform solidification was observed on the S95:T5 coating, which had a higher SFE than the S70:T30:L10 and PET coatings. With lower surface free energies and higher initial grease resistance (S70:T30:L10 and PET), the solidification behavior of the oil was completely different. The coating was evidently capable of repelling the oil, which resulted in a pattern that resembled a doughnut.

Table 7.2 Summary of the oil-substrate interactions at starting point. S denotes starch, T talc and L latex.

	Uncoated reference	S:T 95:5	S:T:L 70:30:10	PET-coated reference
Coat weight, g/m ²	-	8	8	40
OGR (60°C), min	0	90	>1440	>1440
CA (water), °	98	38	68	78
CA (rapeseed oil), °	18	21	23	28
SFE, mN/m	47	45	39	41
	Even grease absorption	Uniform solidification	Uneven solidification	Uneven solidification
Oil on surface (23°C, after 24 h)				

To investigate the influence of corona treatment on the physical properties of HPS-based barrier dispersion coatings, a sample with a S70:T30:L10 coating was measured with AFM. The topography maps (Figure 7.7A–C) revealed that a positive voltage polarity increased the surface roughness more than negative voltage polarity (initial RMS was 48 nm; after treatment with positive or negative voltage polarity the values were 61±18 nm and 68±10 nm, respectively),

although the roughening was overall only moderate. This partly contradicts the results of other studies, which have reported that corona treatment does not cause roughening of a plastic film (Mesic et al. 2005). In the case of negative voltage polarity, the topographical changes were point-form. This observation appears to be linked to the latex particles, since the size of the round objects corresponds to the mean particle size of latex, 160 nm. The latex particles were still in spherical form and obviously not coalesced during drying. This finding might be related to the fact that latex spheres were bound onto talc particles. The adhesion images (Figures 7.7D–F) revealed an increase in tip-substrate interaction (adhesion) after corona treatment. This change was greater in the regions containing talc flakes covered with latex particles. The adhesive properties of the matrix around the talc flakes, which was interpreted to consist of HPS, remained unchanged after corona treatment. The increase in adhesion was ascribed to a minor corona-induced roughening, which partly brought the latex-covered talc particles out of the coating structure. This was also confirmed by XPS analysis that showed increased talc content after corona treatment (see Figure 7.8).

The elasticity and stiffness of the coating were determined by measuring the DMT modulus (Figures 7.7G–I) and the Sneddon modulus (Figures 7.7J–L). Regardless of the voltage polarity, the investigation revealed significant changes in both properties after corona treatment, indicating that the corona treatment makes the surface harder. This observation is also supported by the earlier literature (Goring 1967), which suggests that corona treatment may decrease the tensile properties of wood-based materials, which can be seen as an indication of material hardening. However, the effect of roughening on the elasticity and stiffness cannot be ruled out completely, since it is probable that the observed differences were partly linked to talc particles that the corona treatment brought out from the coating.

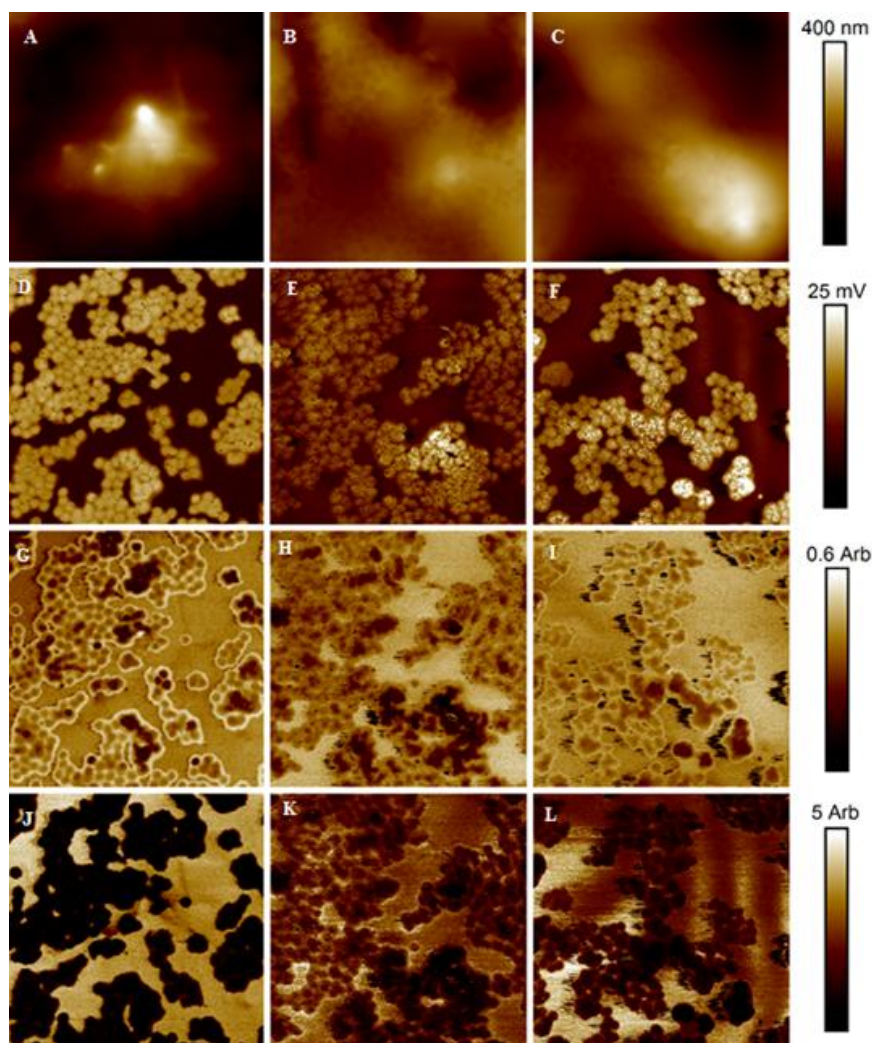


Figure 7.7 AFM images of untreated S70:T30:L10 coating (left), same coating treated with negative voltage polarity (middle) and same coating treated with positive voltage polarity (right). (A–C height; D–F adhesion; G–I DMT modulus; J–L Sneddon modulus)

In order to clarify further the effects of corona-induced surface roughening, the S70:T30 and S70:T30:L10 coatings were analyzed with XPS before and after the corona treatment (Figure 7.8). An increase in the atomic concentrations of silicon and magnesium after corona treatment was registered, which clearly confirms that there was an increase in the content of talc on the surface. Another interesting observation was that the proportion of talc on the coated surface increased regardless of which side of the substrate was treated with corona, which demonstrates the occurrence of reverse-side effects (see Chapter 7.2.2). It was also found that the proportion

of silicon on the surface of the S70:T30 coating increased by approx. 50% after negative corona treatment, but that an even higher concentration of silicon was measured on the latex-containing sample. With positive voltage polarity, the increase in silicon content was higher if latex was present, but no increase was observed on a latex-free surface.

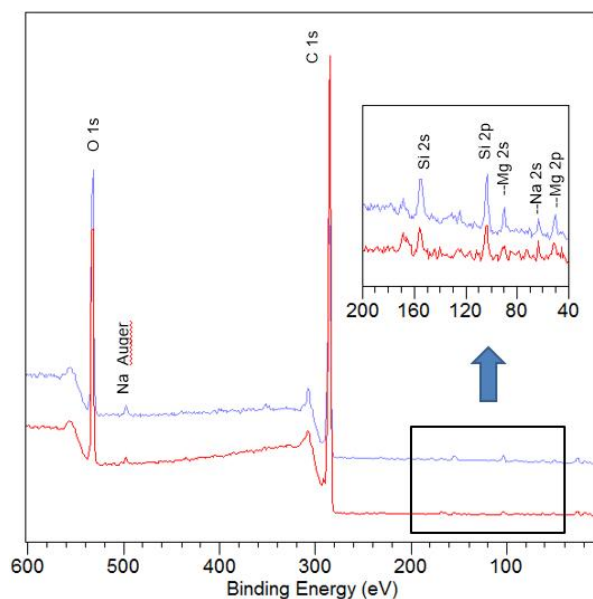


Figure 7.8 XPS survey spectra of the S70:T30:L10 coating before (red line) and after (blue line) negative corona treatment.

Corona treatment increased the oxygen/carbon ratio of the coatings when latex was present, regardless of the voltage polarity (Table 7.3). Without latex, the result was the opposite, but the standard deviation prevents making reliable conclusions about the influence of corona treatment on latex-free surfaces. However, the magnitude of the change corresponded with that reported in earlier literature (Pykönen et al. 2010). The finding that the O/C ratio increases if latex is present demonstrates the high oxidation potential of the latex compared to e.g. pigments. At the same time, the results suggest that the presence of talc in the coating reduces the corona-induced chemical changes. This conclusion is supported by Sidaravicius et al. (2013), who showed that the polarizability of talc is relatively poor compared to that of other typical inorganic minerals used by the paper industry.

Another approach to study the effect of corona treatment on coated surfaces is the determination of their surface free energy (Table 7.3). The surface energy of the non-treated samples

decreased with increasing proportion of talc and with the addition of latex. Both positive and negative corona treatment reduced the surface energy in most cases. The surface energy of the S70:T30 coating remained unchanged after CT, which demonstrates the ability of talc to make the coating more inert. This finding agrees well with the earlier literature, which shows that smaller changes can be expected after corona treatment if the coating contains talc instead of kaolin or a high proportion of latex (Bollström et al. 2011).

Table 7.3 Oxygen to carbon ratios and total surface free energies of HPS-based coatings before and after corona treatment (-400 and +400 W*min/m²).

	S100	S100:L10	S90:T10	S90:T10:L10	S70:T30	S70:T30:L10
<i>O/C ratio</i>						
-400	n.m.	n.m.	n.m.	n.m.	0.51±0.02	0.24±0.02
0	n.m.	n.m.	n.m.	n.m.	0.58±0.02	0.17±0.01
+400	n.m.	n.m.	n.m.	n.m.	0.55±0.02	0.23±0.03
<i>Surface energy, [mN/m]</i>						
-400	46.4	39.3	42.2	41.9	44.6	41.9
0	48.4	45.6	43.1	45.4	44.4	43.2
+400	37.7	45.4	42.3	41.1	44.6	40.4

The contact angle data for rapeseed oil was very similar regardless of the composition of the coating. The effect of corona treatment on the wetting kinetics of rapeseed oil on the S70:T30:L10 coating can be seen in Figure 7.9, which shows that the corona treatment made the coating more oleophobic. Both positive and negative voltage polarities resulted in a similar increase in contact angle, although immediately after the drop had been dispensed, the contact angles were very similar. The influence of corona treatment on the wetting behavior of the oil was revealed after 0.1 s, when the angle reached a plateau on the corona-treated surface. On the non-treated surface, the angle decreased steadily throughout the measurement period. A similar behavior was observed with the other polar probe liquids, water and ethylene glycol. No major differences were observed with the non-polar diiodomethane.

These findings contradict the results of an earlier study, which reported that plasma treatment reduced the contact angle of linseed oil, which is a slightly polar vegetable oil (Pykönen et al. 2010). Possible causes of this difference may be (i.) an oxidation mechanism different from that of direct current corona, (ii.) differences in coating composition, or (iii.) the overemphasized influence of latex, since the distortion caused by changed roughness was ruled out by inspecting the contact angle values after applying a Wenzel roughness correction (for details, see Paper IV).

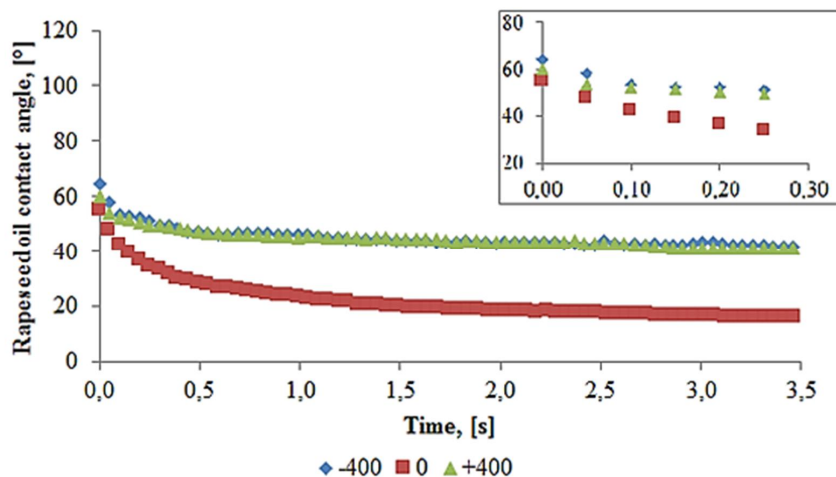


Figure 7.9 Contact angle of rapeseed oil on the S70:T30:L10 coating as a function of time.

The oil and grease resistance of all the studied HPS-based coatings at 60°C was greatly reduced by the corona treatment, regardless of voltage polarity (Figure 7.10). The results suggest that positive treatment is more detrimental to the grease resistance if the coating contains latex, talc or a mixture thereof. The pure HPS coating (S100) suffered more from the negative discharge, but the difference was not significant from the viewpoint of the end-use. The presence of latex in the coating seemed to provide a slight shield against corona treatment with a negative voltage polarity. The samples with 30 pph of talc had an initial grease resistance greater than 24 h, but exposure to corona resulted in a drastic decrease in the grease penetration time. The samples with a lower talc content showed a smaller decrease, but their initial grease resistance was much poorer than that of the coatings containing 30 pph of talc. In many cases, the penetration was limited to very small regions and it seemed to occur through dot-like punctuations. This is a clear indication of strike through and it appears that the deterioration in barrier properties was not linked to any change in chemical composition or physical properties.

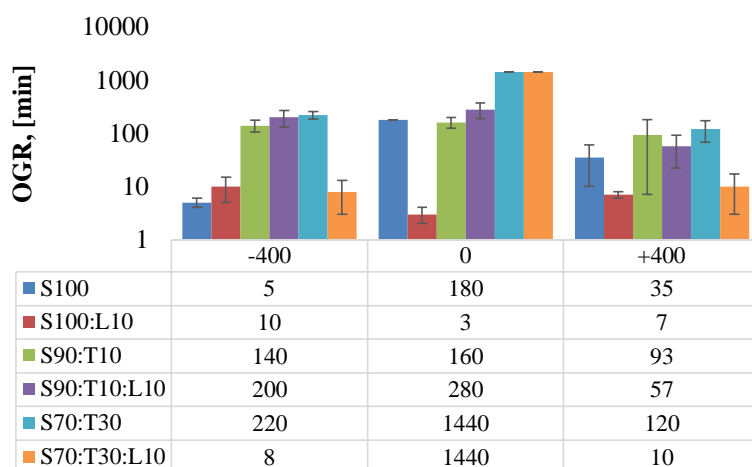


Figure 7.10 Oil and grease resistance of the paperboard samples with different coatings after different corona treatments.

7.2.2 Reverse-side phenomena

Surface energy determinations confirmed that the *coated surface* was affected when the uncoated side was treated with direct current corona (Table 7.4). Significant differences in the occurrence of reverse-side effects were observed between the coatings, and the voltage polarity also affected the results. The initial surface energy of the uncoated surface was lower than that of the coated samples, which was attributed to the presence of hydrophobic sizing agents. Both talc and particularly starch increased the surface energy but, as expected, latex had the opposite effect.

Reverse-side effects of corona treatment decreased the total surface energy of all the coatings with the exception of S70:T30:L10, whose surface energy slightly increased. This behavior was assumed to be a joint effect of the high content of highly inert material (talc) and the presence of latex that has a high polarization potential.

The presence of latex in the coating reduced the basic component of the surface free energy, whereas the presence of talc without latex had the opposite effect. The acidic component remained practically unchanged regardless of the coating composition. Both talc and latex inhibited the reverse-side effects of corona on the dispersive component, although a slight decrease was observed in the case of the S100 coating. A minor alteration in the acid-base polar

component was also observed, but the value was dominated by the presence of latex. This behavior was assumed to be due to the high initial concentration of oxygen molecules in the coating, and this can easily be controlled by adjusting the content of more inert talc in the recipe.

Table 7.4 Surface free energy of the coated side of the substrate after treating the uncoated side with direct current corona.

	Dispersion	Acid-base	Acid	Base	Total, [mN/m]
S100					
<i>Untreated</i>	40.0	9.4	0.9	24.6	49.4
+400 W*min/m ²	35.7	10.6	0.8	36.6	46.3
-400 W*min/m ²	32.2	14.2	1.6	31.4	46.4
S100:L10					
<i>Untreated</i>	39.2	6.4	0.8	11.9	45.6
+400 W*min/m ²	39.6	4.0	1.7	2.4	43.6
-400 W*min/m ²	40.3	3.6	1.2	2.8	43.9
S90:T10					
<i>Untreated</i>	39.5	8.6	0.4	46.5	48.1
+400 W*min/m ²	36.9	10.6	0.8	35.8	47.5
-400 W*min/m ²	38.3	4.8	1.1	5.4	43.1
S90:T10:L10					
<i>Untreated</i>	43.2	2.2	0.4	2.7	45.4
+400 W*min/m ²	41.3	0.6	0.4	0.1	41.9
-400 W*min/m ²	41.7	2.0	1.0	-1.0	43.7
S70:T30					
<i>Untreated</i>	38.3	10.0	0.6	42.6	48.3
+400 W*min/m ²	38.7	7.8	0.4	42.5	46.5
-400 W*min/m ²	37.3	6.6	0.5	23.2	43.9
S70:T30:L10					
<i>Untreated</i>	38.3	1.2	0.1	2.1	39.5
+400 W*min/m ²	41.4	1.4	0.6	-0.9	42.8
-400 W*min/m ²	40.6	2.2	0.9	-1.4	42.8
Reference (uncoated)					
<i>Untreated</i>	37.0	1.2	0.4	-0.9	38.2

Since the reverse-side effects of the corona treatment were surprisingly large, it was reasonable to expect significant changes in the oil-substrate interactions. The contact angles of rapeseed oil on the coated surface after treating the reverse side with corona are shown in Figure 7.11A. The initial contact angle of rapeseed oil on an uncoated and untreated substrate was $24.7 \pm 2.7^\circ$, which was very similar to that on the coated surfaces. The presence of oleophobic latex in the untreated samples had a negligible influence on the contact angle but, after the uncoated side had been corona-treated, the angle increased if the voltage was negative. With positive voltage polarity, the change was negligible when latex was present in the coating. However, without

latex, the positive voltage increased the contact angle even more than negative voltage. The oleophilicity of the S100 and S70:T30 coatings decreased especially after the reverse side was treated with corona. The presence of talc in the latex-free coatings intensified the effect of positive corona treatment on the coated side, suggesting that talc is not able to effectively limit the magnitude of the reverse-side effects.

It can thus be claimed that the reverse-side effects of corona treatment result in larger contact angles of rapeseed oil on HPS-based coatings, although this does not agree with the earlier literature (Pykönen et al. 2010), which states that corona treatment should decrease the contact angle of vegetable oils. However, the contact angle was measured on the treated side of the substrate and the main component of the coating was not starch but an inorganic mineral, both of which make it impossible to make a direct comparison between the present and the earlier results.

Figure 7.11B shows the contact angles on the *uncoated side* after corona treatment on the coated side. In this case, the results agree with the work of Pykönen et al. (2010). Regardless of the coating composition on the coated side, smaller contact angles were recorded on the uncoated reverse side. The voltage polarity had a negligible influence on the contact angle, although it is possible that a negative voltage polarity leads to a slightly greater reduction if the coated side is free of latex. However, the standard deviation of the measurements makes it impossible to draw reliable conclusions.

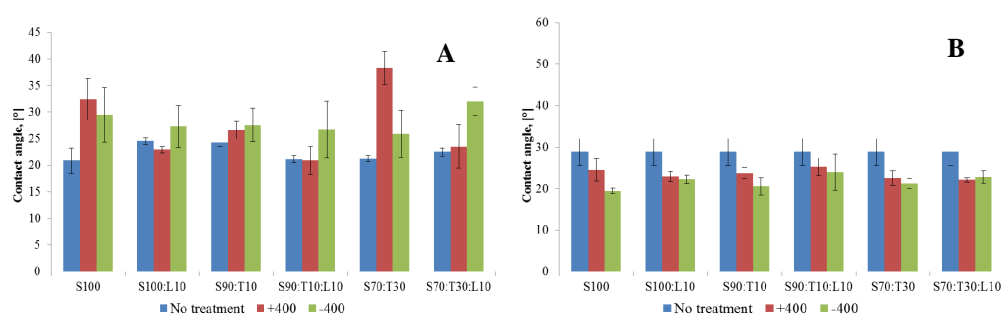


Figure 7.11 Rapeseed oil contact angles (A) on the coated side after treating the uncoated side with corona and (B) on the uncoated side after treating the coated side.

The findings do not exclude the possibility that factor leading to the occurrence of reverse side effects is high surface roughness (Wolf 2007). Figure 7.11B shows clearly that the coating had

no effect on the rapeseed oil contact angles on the uncoated side after treatment of the coated side with corona. Since the roughness of the uncoated side was constant between the samples, it is evident that the chemical composition or topography of the coated side does not affect the reverse-side effects on the uncoated side. Examination of Figure 7.11A shows that differences can arise if the composition of the coating, or its roughness (the PPS roughness of the coatings varied between 7.8–8.9 μm), is changed.

To clarify the role of reverse-side effects on barrier properties, the oil penetration times through samples whose uncoated side was treated with corona were determined (Figure 7.12). Corona treatment impaired the barrier properties of all the samples except for the S100:L10 coating, whose grease resistance was initially poor. The problem was severe with samples containing latex, but a small addition of talc seemed to prevent the total loss of oil and grease resistance. Since the contact angle data showed a slight increase in oil repellence on the coated side after the reverse side had been corona-treated, it seems that the mechanism behind the impaired barrier properties was related to pinholes created by the corona discharge. In addition, the results suggest that the talc in the coating is not able to resist the negative effect of corona if the uncoated side is treated. This indicates that the discharge travels more easily from the uncoated cellulosic surface to the coated side than from the coated to the reverse side. This finding confirms that the porous surface allows the leakage of corona discharge inside the bulk matrix (Väänänen et al. 2010), whereas a denser coating is partly capable to maintain the discharge on the side which it is intended to treat.

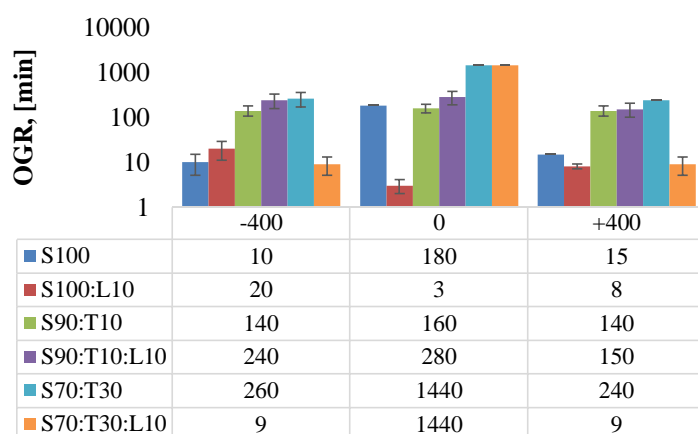


Figure 7.12 Oil and grease resistance of the HPS-based coatings. The uncoated *reverse side* of the sample had been treated with corona. Note logarithmic scale on y-axis.

7.2.3 *Conclusions of the oil and grease resistance of corona-treated substrates*

The results presented in Chapters 7.2.1–7.2.2 illustrate the difficulties related to the corona treatment of HPS-based coatings. Treating the coating layer with a corona discharge significantly impaired its ability to prevent palm kernel oil from penetrating, and the finding was similar when the uncoated side was exposed to a corona discharge. The results agree with an earlier study of corona-treated latex-based dispersion coatings, whose ability to resist the transmission of water vapor decreased after corona treatment (Schumann et al. 2005a). The data thus support the hypothesis that increasing the number of corona treatments that the coated substrate experiences during its converting and finishing processes probably leads to the loss of barrier properties and further to a severely impaired performance in the material's end-use applications.

The experimental substrates should not be judged to be poor substrates without a closer inspection of the reasons behind the loss of barrier properties after corona treatment. All the experimental coatings were relatively thin, which partly explains why they were so sensitive to the corona discharge (Bollström et al. 2011). It must be stressed that the loss of barrier properties was induced by small dot-like pinholes (Figure 7.13) found in the samples regardless of the side of the substrate treated with corona. This finding indicates that optimization of the treatment level may assist in limiting the amount of strike through. However, this is not necessarily the most suitable strategy, since XPS measurements revealed comparatively small differences in the O/C ratios of the coatings, even though the treatment level was quite high. Moreover, the occurrence of reverse-side effects was apparent, which further decreases the effect of corona treatment on the treated side. Another approach is to optimize the composition of the coating so that the detrimental influence of strike through is minimized, which means at least that the pigment content of HPS-based coatings should be high and that the proportion of latex should be carefully optimized. The results also clearly encourage the use of negative voltage polarity, which impaired the OGR less and affected the O/C ratio of the coatings more. In addition, the present study does not exclude the possibility of the wetting phenomena inside the substrate being altered (Väänänen et al. 2010).

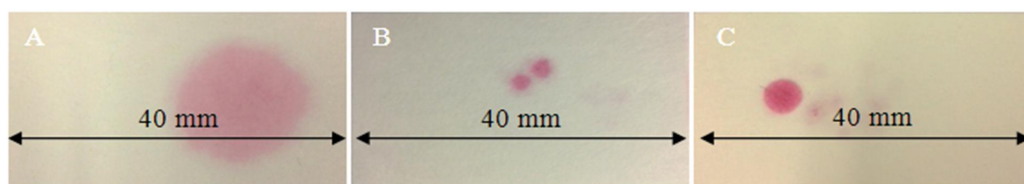


Figure 7.13 Photographs of uncoated sides of samples demonstrating (A) material with poor initial grease resistance, (B) grease penetration through strike through in a material with good initial grease resistance, and (C) perforated material with moderate initial grease resistance.

7.3 Effect of heat exposure and high ambient temperature on coating properties and on oil-substrate interactions (Papers I and VI)

The aim of this chapter is to demonstrate the applicability of barrier coatings in converting processes *from the viewpoint of heat exposure*. The effect on oil-substrate interaction of converting-related heat exposure of dispersion-coated paperboard is discussed in Paper I (HPS-based coatings) and in Paper VI (HPC-based coatings). The heat-induced changes were studied by microscopy and XPS, and by the determination of rapeseed oil contact angles on heat-treated coatings. The effects of mechanical forces on the OGR are discussed separately in Chapter 7.4.

7.3.1 Effect of heat on the chemical composition of coated surfaces

HPS-based dispersion barrier coatings with different proportions of talc (0, 15, and 30 pph) and SB-latex (0 and 10 pph) were used to study the heat-induced changes in the coating layer. SEM images of the cross-sections of coated samples before and after two consecutive heat treatments at 100°C indicated the movement of talc towards the base board, and this was confirmed by XPS analysis on the S70:T30:L10 coating (Figures 7.14–7.15). The atomic concentrations of magnesium and silicate were reduced on the surface after heat exposure, showing that less talc was then present in the uppermost part of the coating. The proportion of carbon increased simultaneously, which indicated an increase in the content of organic compounds. Interestingly, the high-resolution carbon spectra revealed that only the proportion of carbon atoms without oxygen neighbors (C1) increased, whereas the C2 and C3 peaks decreased as a result of heat exposure. It was also found that the signal of the plasmone structure after C1s increased, which confirmed that the increase in C1 was due to aromatic species originating in the latex. However, the proportion of HPS on the surface decreased by only 40% after heating, whereas the

concentration of talc was reduced by approximately 60%. This result agrees with the earlier findings of Dappen (1950), who studied the effect of drying method on the migration of starch binder in pigment coatings. Drying-induced latex migration towards the base paper has also been reported (Kenttä et al. 2006; Sababi et al. 2012).

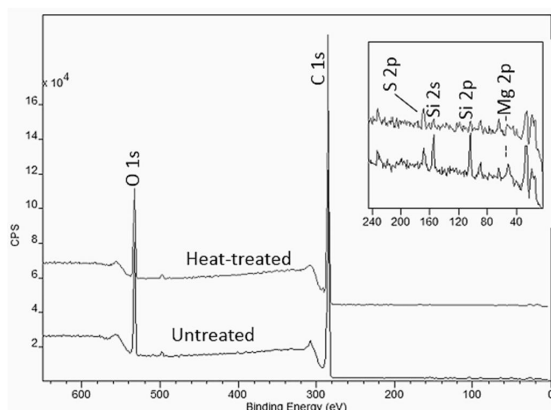


Figure 7.14 XPS wide spectra of untreated and heat-treated samples in which the region with Mg and Si main signals is shown as a zoom-up insert.

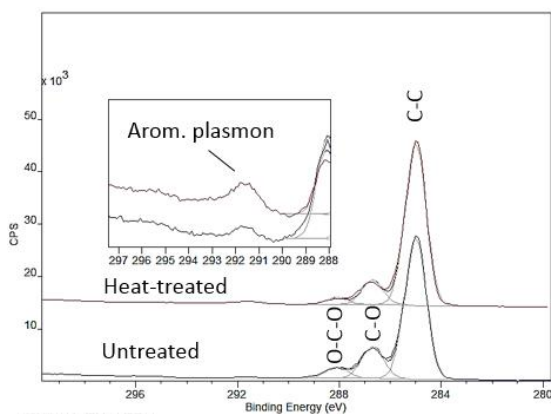


Figure 7.15 XPS carbon C 1s high-resolution spectra of untreated and heat-treated samples. The intensity of the aromatic plasmon agrees with the CC component intensity, confirming that the increase in CC originates mostly from the latex.

7.3.2 Physico-chemical properties of dispersion coatings

The smoothness of dispersion-coated layers was first studied with an optical profilometer. Figure 7.16 shows topographical maps of (A) uncoated substrate, (B) a double-coated plain HPS coating and (C) a double-coated HPS-based composite coating with 30 pph of talc.

Relatively large variations in surface topography were detected, which was attributed to the large thickness variations in the substrate and the coating method used. The roughness of an uncoated sample was in the typical range of SBS boards ($14\ \mu\text{m}$), but coating with a HPS-based dispersion made the surface smoother. The smoothness of a plain HPS coating ($10\ \mu\text{m}$) was, however, very similar to that of talc-containing coatings ($8\text{--}10\ \mu\text{m}$), indicating that a more accurate, ideally *in-situ*, characterization method is needed to distinguish minor differences on coated surfaces, particularly after e.g. heat exposure, as the AFM imaging presented in the next section demonstrated.

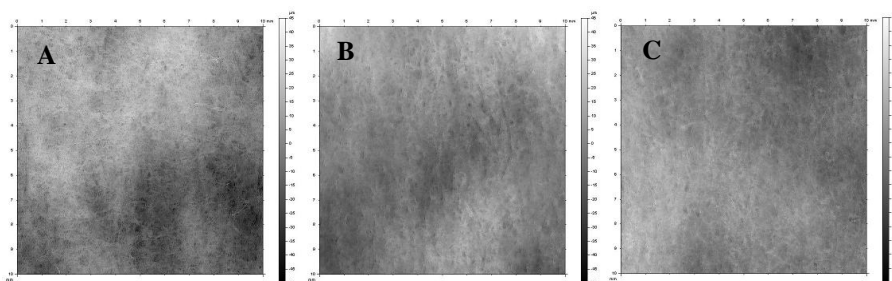


Figure 7.16 Topography images ($10 \times 10\ \text{mm}$) for (A) uncoated base board, (B) a double-coated board with plain HPS, and (C) a double-coated board with HPS and talc in the ratio of 70:30.

Figure 7.17 shows the aspect ratio distribution of the talc, which indicates moderate flakiness. In addition, the particle size distribution of the talc was *bimodal* – flakes large in diameter ($> 10\ \mu\text{m}$) being present among smaller particles (Fig. 7.18). It was found that the smallest particles were needle-like, whereas the largest flakes had a plate-like shape.

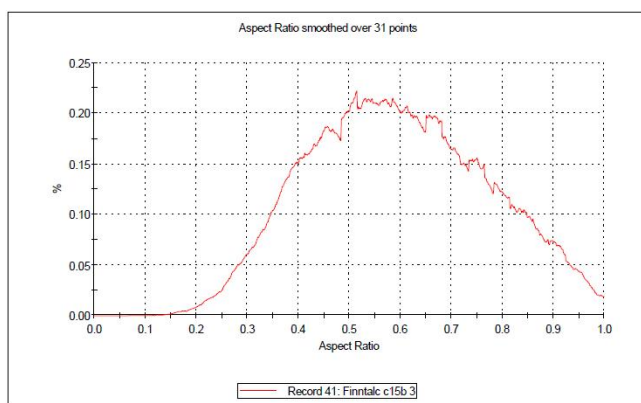


Figure 7.17 Aspect ratio distribution of Finntalc C15B determined with a Malvern Morphologi particle characterization system.

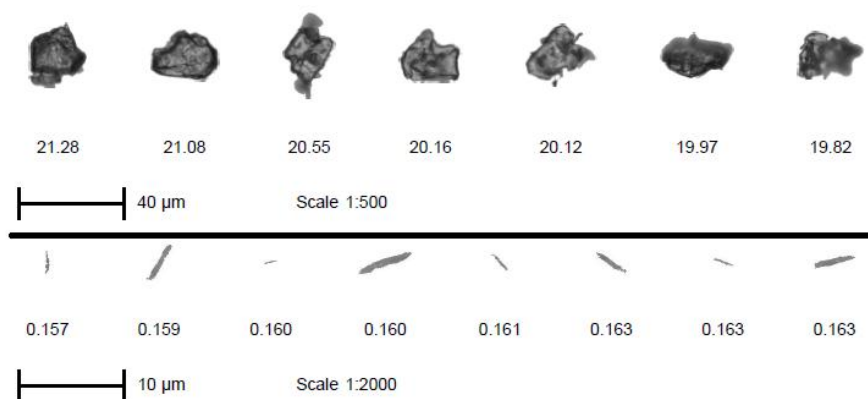


Figure 7.18 Examples of large, plate-like talc particles and smaller, needle-like particles imaged with a Malvern Morphologi particle characterization system.

The suitability of using AFM for imaging composite-type dispersion coatings has earlier been criticized by Vähä-Nissi (1998b), since the area to be measured is often small with respect to the size of pigment particles and the system is thus better suited for nanoscale characterization. To overcome the practical obstacles caused by the dimensions of the pigment particles, relatively large areas ($8 \times 8 \mu\text{m}$) were characterized with AFM in the present study, and particular attention was paid to avoid scanning only the surfaces of the largest pigment particles. The heat-induced morphological changes in the coatings were investigated in the scanning mode (PeakForce QNM mode). The sample was scanned in-situ before, during and after heat treatment at 95°C and both reversible and irreversible changes were observed.

The images A–C in Figure 7.19 show the effect of heat on the topography of the dispersion coating (S70:T30:L10). The local RMS roughness increased from 48 nm to 52 nm during the heating, which was attributed to the formation of small craters on the coated surface. The final roughness after cooling was 53 nm, which indicates that the heat-induced topographical changes in composite dispersion coatings are more or less irreversible and implies that there is a movement of coating components. On the other hand, the changes in adhesion (Figure 7.19D–F) were mostly reversible and largely dependent on the location. The adhesion of the surface generally increased as a result of the heat treatment. These areas were interpreted as consisting of flocculated latex particles. Minor changes in adhesion were observed at 95°C in the darker areas, which was interpreted as being starch. The adhesion of the surface was also reduced in specific locations after cooling, which was assumed to be due to the movement of coating components.

Small changes were found in the DMT modulus of the surface after cooling compared with the initial state (Figure 7.19G–I). The DMT modulus decreased significantly during the heat exposure, which indicates that the surface became more elastic, presumably due to a change in the starch-to-latex ratio on the surface. A similar behavior has earlier been reported in wax-latex systems, although the wax covered the latex particles (Vähä-Nissi 1998b). The elasticity of the background area, which consisted of HPS, remained almost unchanged. The white areas in the middle of images 7.19G and 7.19H were significantly less elastic regions, and probably consisted of talc. These areas were absent after cooling, which suggests that the talc particles were fully covered with polymer after the heat exposure. This interpretation is also supported by XPS results, which showed that the proportion of latex on the surface increased substantially as a result of the heat treatment. The heat-induced changes in DMT modulus were reversible and mainly limited to latex particles.

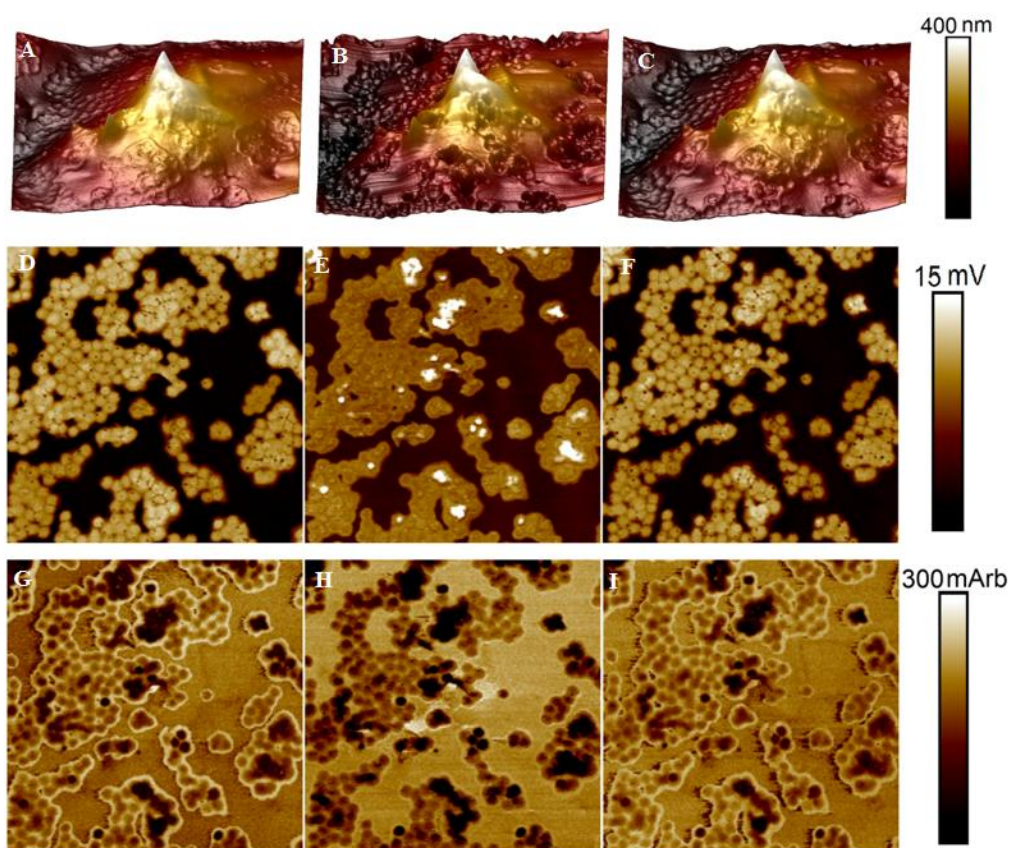


Figure 7.19 3D topography (A–C), 2D adhesion (D–F), and 2D DMT images (G–I) of coating S70:T30:L10 at 25°C before heating (left), after heating at 95°C (middle), and at 25°C after heating and subsequent cooling (right).

SEM images revealed severe coating defects caused by blistering and pinhole formation in both HPS- and HPC-based coatings. In order to obtain barrier properties with dispersion coatings, it is often necessary to apply additional coating layers to cover the defects in the first layer. However, other ways of minimizing the prevalence of coating defects have been considered. For instance, HPC-based coatings had a high tendency to form blisters during drying. The problem was serious with a low pigment content (Figure 7.20A), but an increase in the proportion of talc improved the quality of the coatings substantially (Figure 7.20B). Higher filler proportions also reduced the stickiness of the HPC-based coatings, which, in turn, improved the convertability of the material in press-molding. In addition, the findings highlight the importance of optimizing the drying parameters for dispersions whose dry solids content is low.

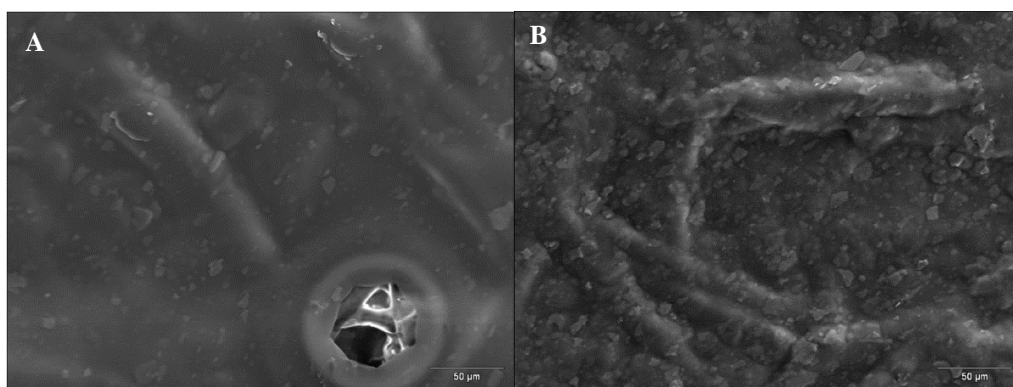


Figure 7.20 SEM images (400x magnification) of HPC-based coatings with (A) low and (B) high pigment proportions. A blister with a diameter of 55 μm can be seen in the lower right-hand corner of Fig. A. The bar size in the figures is 50 μm .

Exposing the dispersion-coated samples to heat revealed the continuation of film formation. In general, HPS-based coatings were smoother than HPC-based coatings, but small pinholes or uneven areas were still visible. A small addition of latex impaired the oil and grease resistance of HPS coatings without a filler (Chapter 7.1.1), which was attributed to impaired film formation due to poor miscibility. The presence of latex, however, induced self-healing of the film on exposure to heat. Similar observation has earlier been reported with waxes by Vähä-Nissi (1998b), who studied the effect of heat treatment on the topography of dispersion coatings consisting of paraffin wax and SB-latex. Figure 7.21A presents a SEM image of the surface of the S70:T30:L10 coating before heat treatment and arrows indicate the observed defects in the coating. After treating the coated sample two minutes at 100°C (Figure 7.21B), no defects were detected and simultaneously the talc particles became less visible, which is another indication

of the movement of latex towards the surface. This alteration in the chemical composition of the surface was earlier indicated by XPS analysis (Chapter 7.3.1).

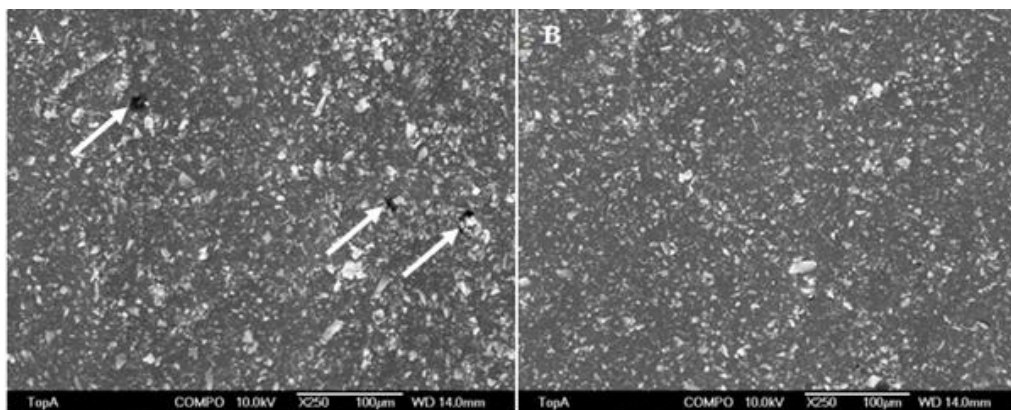


Fig 7.21 Superficial SEM images with a magnification of 250x of coating S70:T30:L10 (A) before and (B) after heat treatment. Defects in the coating are indicated with arrows.

7.3.3 Interactions between substrate and rapeseed oil at elevated temperatures

The heat-induced changes described above, particularly those in the chemical composition of the coated surface, alter the liquid-substrate interactions. To clarify the effect of heat on oil-substrate interactions, the contact angle of rapeseed oil (initial temperature of the oil held at approx. 23°C) was measured at substrate temperatures of 25°C, 50°C, 75°C and 100°C (Figures 7.22–7.23). The heating was carried out by using an electrically heated chamber assembled to the tensiometer. At 25°C, all the contact angles were approximately 22° but the angle increased rapidly with temperature, which suggested an increase in oleophobicity. Based on the results of the XPS measurements (Chapter 7.3.1), it was concluded that this behaviour was induced by the movement of oleophilic talc towards the baseboard and the migration of latex to the outer surface. The typical percentage increase in rapeseed oil contact angle was approx. 20% between 25°C and 100°C. At the most, an increase of 38% was registered on the S70:T30:L10 coating. With talc proportions of 0 and 15 pph, however, the presence of latex led to a smaller increase in contact angle than in the latex-free material, which emphasizes the role of talc for the oleophilic nature of HPS-based composite coatings.

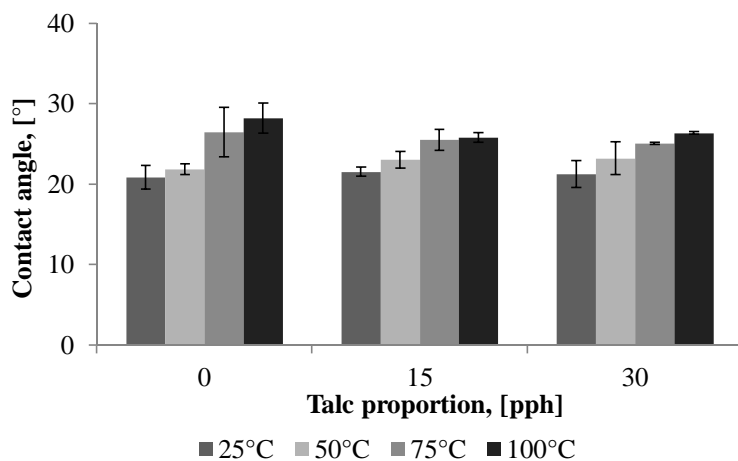


Figure 7.22 Contact angles of rapeseed oil (1 s after dispensing) at different temperatures on latex-free HPS-based coatings. The initial temperature of the oil was constant (23°C) during the experiments.

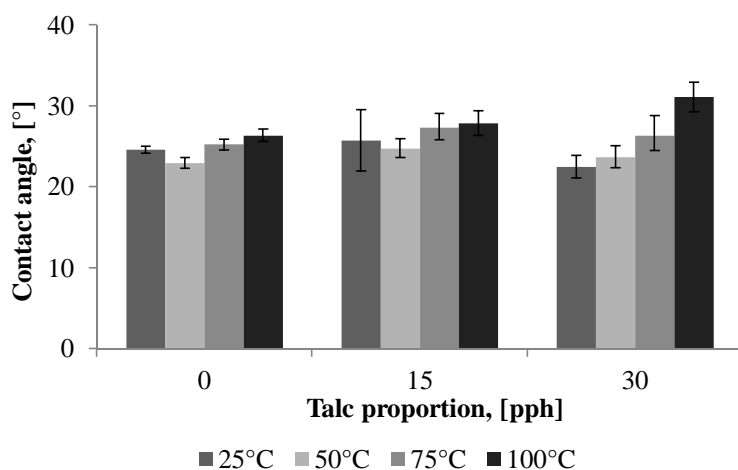


Figure 7.23 Contact angles of rapeseed oil (1 s after dispensing) at different temperatures on latex-containing HPS-based coatings. The initial temperature of oil was constant (23°C) during the experiments.

To study whether the changes occurring in the coating layer were reversible or irreversible, contact angles were measured at 25°C after one and two heat treatments at 100°C (Figure 7.24). When talc was present in the coating, higher contact angles were registered after exposure to heat regardless of whether or not the sample contained latex. When talc was present, the apparent contact angle increased after each heat exposure, which indicates that the coating experienced an irreversible change during the heat treatment. These changes cannot be a

consequence of a change in moisture content, since the samples were conditioned before the contact angle determinations. Taking into account that the oil viscosity was the same in all cases, it is evident that the observed differences are somehow linked to a change in surface composition. Furthermore, a comparison between coatings S100 and S100:L10 revealed that the contact angle of rapeseed oil decreased slightly after thermal treatments. A movement of latex explains the observation in the case of the S100:L10 coating, but the fact that the contact angle also changed on a pure HPS coating indicates that there must have been some other transformation, such as a topographical change or a migration of e.g. AKD from the base board.

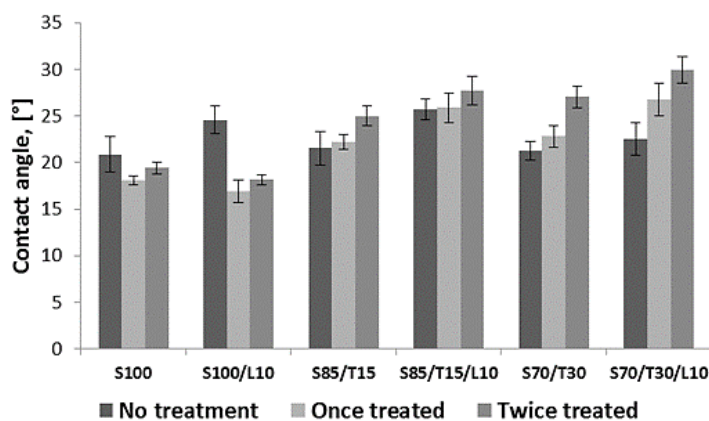


Figure 7.24 Effect of heat treatment on rapeseed oil contact angles on HPS-based coatings. S denotes starch, L latex, and T talc.

7.4 Oil and grease resistance after mechanical processing of paperboard (Paper VI)

The objective of the work presented in Paper VI was to improve the grease-barrier properties of HPC-based coatings by adding talc and simultaneously to maximize the formability of the coated substrate in a press-molding process. The effect of the press-molding process on the grease resistance was evaluated by determining the oil penetration times at corner areas of trays, which were considered to be the most challenging regions, due to the complex shape and large number of creases. The quality of the sealing surface and its effect on barrier properties are also discussed.

HPC is the only film-forming cellulose derivative that provides moderate barrier properties, and is also thermoplastic, biodegradable and recognized to be safe for direct contact with foodstuffs (Krochta and De Mulder-Johnston, 1998). All these properties together make HPC

a fascinating alternative for plastics in packaging applications. However, the mechanical durability of coatings based on cellulose derivatives in creasing and folding processes is poor (Gogoleva 2013), and additives are required to make the coating more flexible (Annushko 2013). In addition, starch films require a large content of a plasticizing agent such as glycerol in order to attain better mechanical properties (Jansson 2003).

7.4.1 Effect of gelatin on the post-creasing OGR of HPS- and HPC-based coatings

The results presented in Figure 7.25 show that the grease resistance of a paperboard with *one* HPC-based coating layer did not differ significantly from that of a HPS-coated sample and that the penetration time increased with increasing gelatin content. After the samples had been creased with a manual creasing machine, the grease resistance deteriorated drastically, although the data suggest that the decrease could partly be compensated for by the addition of a small amount of gelatin. Even though the grease resistance of single-coated paperboards was poor, regardless of whether or not the sample was creased, the results are in line with earlier reports in the literature. For instance, Billmers et al. (2004) stated that gelatin could be used not only to enhance the grease resistance of starch-based coatings, but also to reduce their brittleness.

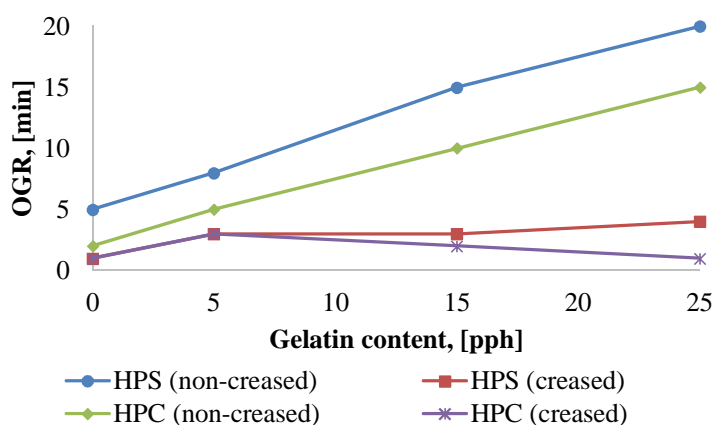


Figure 7.25 Oil and grease resistance of *single* HPS/gelatin and HPC/gelatin coating layers (coat weight 8–10 g/m²) as a function of gelatin content.

7.4.2 OGR of press-formed trays

OGR values after a creasing process do not provide sufficient information, since the paperboard also experiences mechanical forces in the molding process. To study the grease resistance

properties of ready-made trays, *double-coated* boards with HPC-based barrier layers were converted into trays and the grease resistance of the corner regions were determined. The oil penetration times through unconverted materials varied between 2 and 25 minutes (Figure 7.26), which was considerably shorter than that of the HPS-based coatings. The oil and grease resistance of the HPC-based coatings was not greatly affected by the coat weight, but the introduction of 20–30 pph of talc resulted in a substantial increase in the penetration time of palm kernel oil. Again, it was found that adding gelatin to HPC improved both the grease resistance of both unconverted and converted material at the corner areas. The compatibility of talc and gelatin in terms of oil-barrier properties remained unclear, since the OGR value of sample with 10 pph of talc was shorter than that of the H100:G5 coating. It is also worth mentioning that synthetic polymers may also improve the barrier properties and convertability of bio-based coatings (Tanninen et al. 2014).

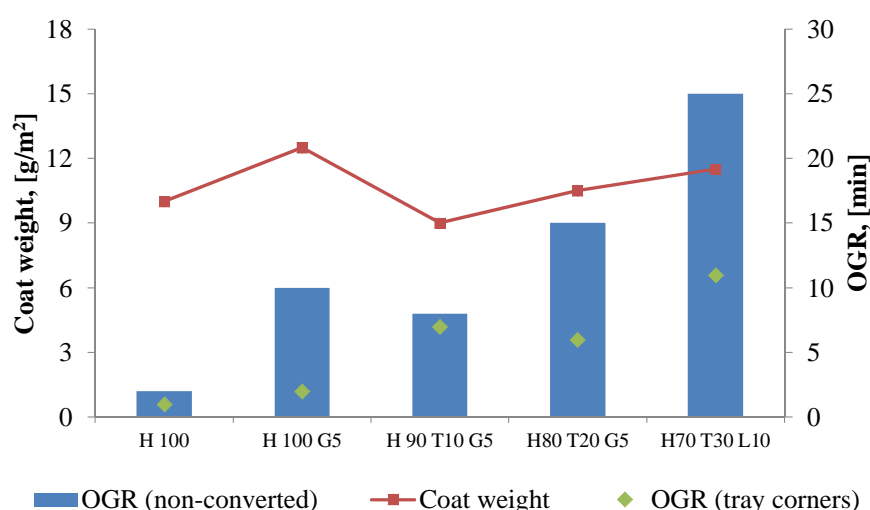


Figure 7.26 Coat weight (g/m^2) and penetration times of palm kernel oil through non-converted and converted samples. H denotes HPC, G gelatin, T talc and L latex.

The barrier properties of the tray can also be examined from other perspectives. The creases and wrinkles in the rim area of press-formed trays can be 400 μm deep (Leminen et al. 2015), although attempts are usually made to achieve high smoothness of the sealing surface and creases with a depth of up to 150 μm are not considered detrimental. Indeed, the flatness of the tray flange is an important property for achieving an effective and protective lid, and it improves the visual appearance of the package. Figure 7.27A shows a cross-sectional micrograph of a

poorly formed crease in the sealing surface of a PET-coated tray (commercial reference), which increases the risk of leakages if the tray has a lid. However, the creases were difficult to locate even with a microscope in the trays manufactured from board having experimental HPC-based coatings (Fig. 7.27B). The difference in coat weight and the stickier nature of the HPC explain the observed differences at least partly but, most importantly, the findings demonstrate that the convertability of HPC-based barrier dispersion coatings is not necessarily a major problem, but that more attention should be paid to the maximization of the barrier properties. The barrier properties of HPC-based coatings might be adequate only for short-term end-use applications such as fast food packages.

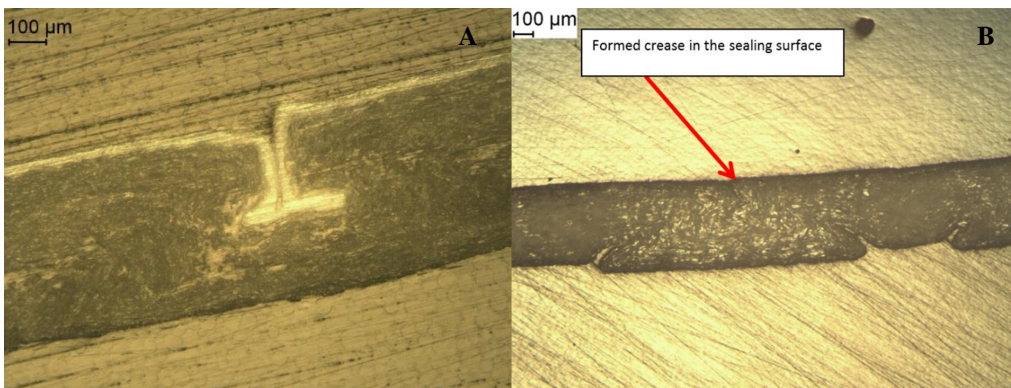


Figure 7.27 Cross-sectional micrographs of a crease formed in (A) commercial PET-coated paperboard and in (B) experimental material with H70:T30:L10 coating.

8 CONCLUDING REMARKS

The purpose of this work was to clarify the effects of converting and finishing processes on the interactions between edible oils and dispersion-coated paperboard. Particular attention was paid to the determination of the roles of the pigment content and the content of synthetic polymer, including the influence of oil properties on the oil penetration behavior. When the oil repellence of dispersion-coated surfaces and the oil resistance of the packaging material were compared, it became evident that these two properties are completely unconnected, since a higher contact angle of the oil did not lead to a longer penetration time. This suggests that the tortuosity probably dominated the oil barrier properties of the material. Consequently, preventing damage of the coating layer in finishing and converting processes is essential and process optimization is required when plastic-coated materials are replaced with highly bio-based substrates.

Coatings were characterized by e.g. microscopic analyses, oil and grease resistance experiments and contact angle determinations. It was shown that both corona treatment and heat exposure lead to alterations in the chemical composition of the surface and in physical properties such as its topography. Treating the coated substrates with corona resulted in strike through and unintentional reverse-side effects, but heat-induced changes are not necessarily detrimental to barrier properties, since the migration of the synthetic polymer towards the outer surface may reduce the number of pinholes and increase the oil contact angles. On the other hand, this indicates that the feasibility of using completely bio-based coatings is limited, since defects such as blistering were observed in coatings consisting solely of biopolymers. The results also support the use of pigments such as talc in the coating, not only because it gives better barrier properties, but also due to their stabilizing effect on corona treatment and reduced stickiness.

The penetration characteristics of vegetable oils were studied by CLSM. Coconut oil showed solidification behavior and accumulation inside the coating layer, whereas rapeseed oil spread more evenly inside the packaging material. It was also shown that the penetration time of pure oils through the paperboard was longer than that of the oil blends, and that an increase in the pigmentation level prolonged the penetration time of oils whose saturated fat content was high. The results thus suggest that there are differences in the diffusion mechanisms of unsaturated and saturated fats. These findings confirm that the transition from unsaturated fats to vegetable oils in the food industry sets new requirements for barrier materials.

The results obtained have increased the knowledge of the feasibility of using highly bio-based barrier dispersion coatings in food packaging applications. Interlinking the initial grease resistance and post-converting barrier properties makes it possible not only to evaluate the applicability of the packaging material for end-use purposes but also to optimize the suitability for converting and finishing processes of novel packaging materials. The coating formulations developed may have a potential in many commercial sustainable packaging applications where moderate oil and grease resistance is needed together with coating simplicity. This study, however, leaves a topic for wider characterization of oil-induced swelling and solubility behavior of bio-based dispersion barrier coatings. In addition, there are still few technical challenges such as blistering and blocking to be solved. As a whole, the potential for implementing these coating formulations in industrial production can still be considered promising, since the coating components studied are commercial products, their price in most cases is attractive and their presence in food packages has mostly been approved.

REFERENCES

Al-Turaif, H.-A. and Bousfield, D. W. (2005). The Influence of Pigment Size Distribution and Morphology on Coating Binder Migration. *Nordic Pulp and Paper Research Journal*, 20(3), pp. 335–344.

Andersson, C. (2001). *Polymer Interdiffusion in Dispersion Coatings and its Relation to Barrier Properties*, Licentiate thesis, Karlstad University, Sweden. 82 p.

Andersson, C., Järnström, L. and Hellgren, A.-C. (2002a). Effects of carboxylation on polymer Interdiffusion and water vapor permeability in latex films. *Nordic Pulp and Paper Research Journal*, 17(1), pp. 20–28.

Andersson, C., Erntsson, M. and Järnström, L. (2002b). Barrier properties and heat sealability/failure mechanisms of dispersion-coated paperboard. *Packaging Technology and Science*, 15(4), pp. 209–224.

Annushko, A. (2013). *Gelatin as an additive in bio-based barrier films*, Master's thesis, Lappeenranta University of Technology, Finland. 94 p.

Anon. (2006). *Consumers and Ready-to-Eat Meals: A Global ACNielsen Report*, ACNielsen, USA, pp. 1–8.

Aulin, C., Shchukarev, A., Lindqvist, J., Malmström, E., Wågberg, L. and Lindström, T. (2008). Wetting kinetics of oil mixtures on fluorinated model cellulose surfaces. *Journal of Colloid and Interface Science*, 317(2), pp. 556–567.

Backfolk, K., Andersson, C. and Peltonen, J. (2006). Association between a sodium salt of a linear dodecylbenzene sulphonate and a non-ionic fatty alcohol ethoxylate surfactant during film formation of styrene/butadiene latex. *Colloids and Surfaces A: Physicochemical and Engineering Aspects*, 291(1–3), pp. 38–44.

Backfolk, K., Sidaravicius, J., Sirviö, P., Maldzius, R., Lozovski, T. and Rosenholm, J. B. (2010). Effect of base paper grammage and electrolyte content on electrical and dielectric properties of coated papers. *Nordic Pulp and Paper Research Journal*, 25(3), pp. 319–327.

Billmers, R. L., Mackevitz, V. L. and Trksak, R. M. (2004). Protein and starch surface sizings for oil and grease resistant paper, US Patent 6,790,270 B1, USA, September 14.

Black, E. P., Duling, I. N., Talbot, A. F. and Peterkin, M. E. (1970). *Plastic coatings from polymer-in-wax dispersions*. In: 25th TAPPI Plast. Pap. Conference, pp. 141–153.

Blackley, D. C. (1997). *Polymer Latices Science and Technology Volume 3: Applications of latices*. Springer, Netherlands. 655 p.

Bloembergen, S., Santos, M. P., Greenall, P., DeJong, R., Shin, J. Y., Jones, N. and Lee, I. (2014). The effects of biolatex binders on the dynamic water retention properties of paper coating formulations. *O Papel*, 75(3), pp. 55–65.

Bollström, R., Tuominen, M., Määttä, A., Peltonen, J. and Toivakka, M. (2011) *Top layer coatability on barrier coatings*. In: 11th TAPPI PaperCon Conference, Cincinnati, OH, USA, pp. 281–291.

Bollström, R., Nyqvist, R., Preston, J., Salminen, P. and Toivakka, M. (2013). Barrier properties created by dispersion coating. *TAPPI Journal*, 12(4), pp. 45–51.

Brimen, J. S. and Proverb, R. J. (1991). SIMS imaging of paper surfaces: Part 2. Distribution of organic surfactants. *Nordic Pulp and Paper Research Journal*, 6(4), pp. 177–183.

Bristow, J. A. (1967). Liquid Absorption into Paper during Short Time Intervals. *Svensk Papperstidning*, 70(19), pp. 623–629.

Bristow, J. A. (1971). The swelling of paper during the sorption of aqueous liquids. *Svensk Papperstidning*, 74(20), pp. 645–652.

Bristow, J. A. (1972). Swelling of fiber building boards on immersion in water. *Svensk Papperstidning*, 75(21), pp. 847–852.

Bristow, J. A. (2016). Private communication, 23 June.

Carne, T. (1997). *Användning av talk i barriärbestrykningar*, Master's Thesis, Åbo Akademi, Finland. 81 p.

Cernakova, L., Staelh, P., Kovacik, D., Johansson, K. and Cernak, M. (2006). *Low cost high-speed plasma treatment of paper surfaces*. In: 9th TAPPI Advanced Coating Fundamentals Symposium, Turku, Finland. 11 p.

Cheong, L.-Z., Zhang, H., Xu, Y. and Xu, X. (2009). Physical characterization of lard partial acylglycerols and their effects on melting and crystallization properties of blends with rapeseed oil. *Journal of Agricultural and Food Chemistry*, 57, pp. 5020–5027.

Csuros, Z., Bozzay, J. and Zsoldos, B. (1968). Rheologische untersuchen kaolinhaltiger dispersionen. *Periodica Polytechnica: Chemical Engineering*, 12(4), pp. 381–394.

Dappen, J. W. (1950). *The Distribution of Starch in Clay Coatings*, Dissertation, The Institute of Paper Chemistry, Appleton, WI, USA. 118 p.

De Gennes P. G., Brochard-Wyart F. and Quere, D. (2004). *Capillarity and Wetting Phenomena*, Springer, New York, NY, USA. 292 p.

De Marco, E., Savarese, M., Parisini, C., Battimo, I., Falco, S. and Sacchi, R. (2007). Frying comparison of a sunflower/palm oil blend in comparison with pure palm oil. *European Journal of Lipid Science and Technology*, 109, pp. 237–246.

Dutt, D., Mishra, A. K., Kumar, A. and Mishra, N. C. (2012). Cost reduction and upgrading of basic properties of absorbent-grade paper. *Bioresources*, 7(3), pp. 3125–3131.

Eklund, D. and Salminen, P. (1987). Water sorption in paper during short times. *Appita Journal*, 40(5), pp. 340–346.

Elliot, J. L. (1938). Coated materials and to processes for producing the coating, US Patent 2116066A, May 3.

Endres, I. and Tietz, M. (2007). Blade, film and curtain coating techniques and their influence on paper surface characteristics. *TAPPI Journal*, 6(11), pp. 24–32.

Esteban, B., Riba, J.-R., Baquero, G., Rius, A. and Puig, R. (2012). Temperature dependence of density and viscosity of vegetable oils. *Biomass and Bioenergy*, 42, pp. 164–171.

Fayoux, S. C., Seuvre, A.-M. and Voilley, A. J. (1997). Aroma transfers in and through plastic packagings: Orange juice and d-limonene. A review: Part 1. Orange juice aroma sorption. *Packaging Technology and Science*, 10, pp. 69–82.

Finch, C. A. (2001). Applications of latices in the paper industry. In: Warson, H. and Finch, C. A. Eds. *Applications of Synthetic Latices, Vol. 3 Latices in Diverse Applications*, John Wiley & Sons Ltd., UK, pp. 1222–1270.

Földes, E., Tóth, A., Kálmán, E., Fekete, E. and Tomasovszky- Bobák, Á. (2000). Surface changes of corona-discharge-treated polyethylene films. *Journal of Applied Polymer Science*, 76, pp. 1529–1541.

Gainé, W. E. (1853). Treating or preparing paper, Patent GB 2834, December 6.

Galanti, F., Gallone, G. and Carpi, F. (2012). Effects of corona treatment on electrical and mechanical properties of a porous dielectric elastomer. *IEEE Transactions on Dielectrics and Electrical Insulation*, 19(4), pp. 1203–1207.

Giesy J. P. and Kurunthachalam K. (2002). Perfluorochemical surfactants in the environment. *Environmental Science & Technology*, 36(7), pp. 146A–152A.

Gogoleva, E. (2013). *Effects of converting on barrier properties of multi-component coatings*, Master's thesis, Lappeenranta University of Technology, Finland. 53 p.

Goring, D. A. I. (1967). Surface modification of cellulose in a corona discharge. *Pulp and paper magazine of Canada*, 68(8), pp. T372–T376.

Harrod, S. (2011). *The Future of Functional Additives and Barrier Coatings for Paper and Board to 2016*. Pira International Ltd, Surrey, UK. 56 p.

Hedenqvist, M. and Gedde, U. W. (1996). Diffusion of small-molecule penetrants in semicrystalline polymers. *Progress in Polymer Science*, 21(2), pp. 299–333.

Hernandez-Muñoz, P., Catala, R. and Gavara, R. (1999). Effect of sorbed oil on food aroma loss through packaging materials. *Journal of Agricultural and Food Chemistry*, 47(10), pp. 4370–4374.

- Hirvikorpi, T., Vähä-Nissi, M., Harlin, A., Marles, J., Miikkulainen V. and Karppinen, M. (2010). Effect of corona pre-treatment on the performance of gas barrier layers applied by atomic layer deposition onto polymer-coated paperboard. *Applied Surface Science*, 257, pp. 736–740.
- Hoyland, R. W. (1978). Fibre-water interactions in paper-making. *Technical Division BPBIF*, pp. 557–577.
- Jansson, A. (2003). *Barrier and mechanical properties of starch films based on regular potato starches and high amylose potato starches*, Licentiate thesis, Karlstad University, Sweden. 39 p.
- Jansson, A. (2006). *Modified starches in aqueous and plastisol coating*, Dissertation, Karlstad University, Sweden.
- Johansson, L.-S. and Campbell, J. (2004). Reproducible XPS on biopolymers: cellulose studies. *Surface and Interface Analysis*, 36(8), pp. 1018–1022.
- Kandlikar, S. G. and Steinke, M. E. (2002). Contact angles and interface behavior during rapid evaporation of liquid on a heated surface. *International Journal of Heat and Mass Transfer*, 45, pp. 3771–3780.
- Karhu, A. (2012). *Biobased Polymers in Dispersion Coating*, Master's thesis, Lappeenranta University of Technology, Finland. 98 p.
- Kenttä, E., Pöhler, T. and Juvonen, K. (2006). Latex uniformity in the coating layer of paper. *Nordic Pulp and Paper Research Journal*, 21(5), pp. 665–669.
- Khan, M. I. and Nasef, M. M. (2009). Spreading behaviour of silicone oil and glycerol drops on coated papers. *Leonardo Journal of Sciences*, 8, pp. 18–30.
- Kimpimäki, T. and Savolainen, A. (1997). Barrier dispersion coating of paper and board. In: Brander, J. and Thorn, I. Eds. *Surface Applications of Paper Chemicals*, Chapman & Hall, London, pp. 208–228.
- Kimpimäki, T. (1998). Dispersion coating and product applications. In: Savolainen, A. Ed., *Papermaking Science and Technology*, Book 12, Fapet Oy, Jyväskylä, pp. 81–122.
- Koivula, H., Alm H. K. and Toivakka M. (2011). Temperature and moisture effects on wetting of calcite surfaces by offset ink constituents. *Colloids and Surfaces A: Physicochemical and Engineering Aspects*, 390, pp. 105–111.
- Koivula, H., Jalkanen, L., Saukkonen, E., Ovaska, S.-S., Lahti, J., Christophliemk, H. and Mikkonen, K. S. (2015). Machine-coated starch-based dispersion coatings prevent mineral oil migration from paperboard. *Progress in Organic Coatings*, 99, pp. 173–181.
- Krochta, J. M. and De Mulder-Johnston, C. (1997). Edible films solve problems. *Journal of Food Technology*, 51(2), pp. 60–74.

Kugge, C. and Johnson, B. (2008). Improved barrier properties of double dispersion coated liner. *Progress in Organic Coatings*, 62, pp. 430–435.

Kuusipalo, J. (2003). Characterization and converting of dispersion and extrusion coated high-density papers. *Paper, Film and Foil Converter*, 77(5), pp. 68–70.

Lahti, J. and Tuominen, M. *The effects of corona and flame treatment: Part 1. PE-LD coated packaging board*. In: 11th TAPPI European Place Conference, Athens, Greece, pp. 1446–1487

Lange, J., Pelletier, C. and Wyser, Y. (2002). Novel method for testing the grease resistance of pet food packaging. *Packaging Technology and Science*, 15(2), pp. 65–74.

Leminen, V., Mäkelä, P., Tanninen, P. and Varis, J. (2015). Leakproof heat sealing of paperboard trays - effect of sealing pressure and crease geometry. *Bioresources*, 10(4), pp. 6906–6916.

Lindell, H., Nevalainen, K., Laitinen, R., Kauri, T. and Peltovuori, M. (2011). *Paperboard as a substrate for extrusion coating*. In: 13th TAPPI European Place Conference, Bregenz, Austria, pp. 800–817.

Mali, S., Grossman, M. V. E., Garcia, M. A., Martino, M. N. and Zaritzky, N. E. (2005). Mechanical and thermal properties of yam starch films. *Food Hydrocolloids*, 19(1), pp. 157–164.

Mesic, B., Lestelius, M., Engström, G. and Edholm, B. (2005). Printability of PE-coated paperboard with water-borne flexography: effects of corona treatment and surfactants addition. *Pulp and Paper Canada*, 106(11), pp. 36–41.

Mielonen, K., Ovaska, S.-S. and Backfolk, K. (2015). *Potential of coating comprising hydroxypropylated starch for dye-based inkjet printing*. In: NIP31 & Digital Fabrication, Society for Imaging Science and Technology, Portland, OR, USA, pp. 462–466.

Mills, C. K. (1908). Waxing composition for paper and process of preparing the same, Patent GB190809653A, August 20.

Morabito, P. (2004). Barrier coatings for oil and grease resistance, US Patent Application 2004/0241475 A1, December 2.

Ninness, B., Welsch, G., Ventresca, D. and Williams, D. (2011). *Aqueous glue setting in double-coated paperboard systems - The impact of application system and individual coating layer thickness on glue bond formation*. In: TAPPI Papercon 2011, Covington, KY, USA, pp. 1751–1769.

Noureddini, H., Teoh, B. C. and Clements, L. D. (1992). Viscosities of vegetable oils and fatty acids. *Journal of the American Oil Chemists' Society*, 69(12), pp. 1189–1191.

Näsman, M. (2000). *Filmbildning av styren-butadien latex*, Master's thesis, Åbo Akademi University, Turku, Finland.

O'Brien, R. C. (1995). *Fats and Oils: Formulating and Processing for Applications*, Lancaster, pp. 5–7.

Oberndorfer, J. and Greenall, P. (2011). *Coating & print performance of biobased latex in European graphic papers*. In: TAPPI Papercon 2011, Covington, KY, USA, pp. 1136–1151.

Olafsson, G. and Hildingsson, I. (1995). Sorption of fatty acids into low-density polyethylene and its effects on adhesion with aluminum foil laminated packaging material. *Journal of Agricultural and Food Chemistry*, 43(2), pp. 306–312.

Oliver, J. F. and Forsyth, R. C. (1990). A dynamic liquid sorption apparatus for studying interactions of microscopic drops in situ on porous substrates. *Colloids and Surfaces*, 43(2–4), pp. 295–305.

Olsson, E., Johansson, C., Larsson, J. and Järnström, L. (2014a). Montmorillonite for starch-based barrier dispersion coating: Part 2. Pilot trials and PE-lamination. *Applied Clay Science*, 97–98(August 2014), pp. 167–173.

Olsson, E., Johansson, C. and Järnström, L. (2014b). Montmorillonite for starch-based barrier dispersion coating: Part 1. The influence of citric acid and poly(ethylene glycol) on viscosity and barrier properties. *Applied Clay Science*, 97–98(August 2014), pp. 160–166.

Ovaska, S.-S. and Backfolk, K. (2013). *Optimizing grease resistance of dispersion barrier coatings for heterogeneous grease mixtures*. In: PTS Coating Symposium, Munich, Germany, pp. 412–423.

Perng, Y.-S. and Wang, E. I.-C. (2012). Optimization of handsheet greaseproof properties: The effects of furnish, refining, fillers and binders. *Bioresources*, 7(3), pp. 3895–3909.

Powers, P. O. and Pflum J. F. (1961). Hydrocarbon resins in paper coatings. *Industrial and Engineering Chemistry*, 53(5), pp. 371–374.

Prabhu, K. N., Fernandes, P. and Kumar, G. (2009). Effect of substrate surface roughness on wetting behaviour of vegetable oils. *Materials & Design*, 30, pp. 297–305.

Pykönen, M. (2010). *Influence of Plasma Modification on Surface Properties and Offset Printability of Coated Paper*, Dissertation, Åbo Akademi University, Finland. 62 p.

Pykönen, M., Silvaani, H., Preston, J., Fardim, P. and Toivakka, M. (2010). Influence of plasma activation on absorption of offset ink components into pigment-coated paper. *Nordic Pulp and Paper Research Journal*, 25(1), pp. 93–99.

Ramsey, S. W. (2012). *Using GRAS bio-based materials in UV-cured coatings*. In: 39th Annual International Waterborne, High-Solids, and Powder Coatings Symposium, Lancaster, PA, USA, pp. 192–202.

Rissa, K., Lepistö, T., Vähä-Nissi, M. and Savolainen, A. (1999). *Application of atomic force microscopy in pigment and dispersion coating analyses*. In: 1999 TAPPI Advanced Coating Fundamentals Symposium, Toronto, ON, Canada, pp. 175–189.

Rissa, K., Lepistö, T., Vähä-Nissi, M., Lahti, J. and Savolainen, A. (2000). Orientation of talc particles in dispersion coatings. *Nordic Pulp and Paper Research Journal*, 15(5), pp. 357–361.

Rojas, O. (2009). *Use of complex fluids for enhanced cellulosic pretreatment*, Final project report, The Southeastern Sun Grant Center. 13 p.

Ronka, S. J. (2010). Coated recyclable paper or paperboard and methods for their production, Patent WO/2010/052571, May 14.

Rosenholm, J. B. (2015). Liquid spreading on solid surfaces and penetration into porous matrices: Coated and uncoated papers. *Advances in Colloid and Interface Science*, 220(June 2015), pp. 8–53.

Roth, W. B. and Mehlretter, C. L. (1967). Some properties of hydroxypropylated amylo maize starch films. *Journal of Food Technology*, 21, pp. 72–74.

Rousu, S., Pfau, A., Schröder, V., Wirth, T., Lindström, M., Eklund, D. and Gane, P. (2002). Influence of latex – oil interactions on offset ink setting and component distribution on coated paper. *Journal of Graphic Technology*, 1(2), pp. 45–56.

Sababi, M., Kettle, J., Rautkoski, H., Claesson, P. M. and Thormann, E. (2012). Structural and nanomechanical properties of paperboard coatings studied by peak force tapping atomic force microscopy. *ACS Applied Materials & Interfaces*, 4(10), pp. 5534–5541.

Salminen, P., Yang, A., Kritzing, J., Bauer, W. and Preston, J. (2010). *The influence of application system on the structure of coating layer*. In: TAPPI PaperCon 2010, Atlanta, GA, USA, pp. 432–456.

Schoelkopf, J., Gane, P. A. C. and Ridgway C. J. (2000). Influence of inertia on liquid absorption into paper coating structures. *Nordic Pulp and Paper Research Journal*, 15(5), pp. 422–430.

Schoelkopf, J., Gane, P. A. C., Ridgway, C. J. and Matthews, G. P. (2002). Practical observation of deviation from Lucas-Washburn scaling in porous media. *Colloids and Surfaces A*, 206(1–3), pp. 445–454.

Schuman, T., Wikström, M. and Rigdahl, M. (2004a). Dispersion coating with carboxylated and cross-linked styrene–butadiene latices: Part 1. Effect of some polymer characteristics on film properties. *Progress in organic coatings*, 51(3), pp. 220–227.

Schuman, T., Wikström, M. and Rigdahl, M. (2004b). Dispersion coating with carboxylated and cross-linked styrene–butadiene latices: Part 2. Effects of substrate and polymer characteristics on the properties of coated paperboard. *Progress in Organic Coatings*, 51(3), pp. 228–237.

Schuman, T., Adolfsson, B., Wikström, M. and Rigdahl, M. (2005a). Surface treatment and printing properties of dispersion-coated paperboard. *Progress in Organic Coatings*, 54(3), pp. 188–197.

Schuman, T., Karlsson, A., Larsson, J., Wikström, M. and Rigdahl, M. (2005b). Characteristics of pigment-filled polymer coatings on paperboard. *Progress in Organic Coatings*, 54(4), pp. 360–371.

Schuster, E., Eckardt, J., Hermansson, A. M., Larsson, A., Lorén, N., Altskär, A. and Ström, A. (2014). Microstructural, mechanical and mass transport properties of isotropic and capillary alginate gels. *Soft matter*, 10(2), pp. 357–366.

Sculley, J. D. and Bruno, M. F. (1968). Coated polyolefin film structure and process of preparation thereof, Patent US3397163 A, August 13.

Seguchi, M. (1984). Oil-binding capacity of heat-treated wheat starch. *Cereal Chemistry Journal*, 61(3), pp. 248–250.

Shahin, M. M. (1966). Mass-spectrometric studies of corona discharges in air at atmospheric pressures. *Journal of Chemical Physics*, 45(7), pp. 2600–2605.

Shahin, M. M. (1969). Nature of charge carriers in negative coronas. *Applied Optics*, 8, pp. 106–110.

Shankar, A., Xiao, J. and Ducatman A. (2001). Perfluoroalkyl chemicals and chronic kidney disease in US adults. *American Journal of Epidemiology*, 174(8), pp. 893–900.

Sidaravicius, J., Lozovski, T., Jurksus, J., Maldzius, R., Backfolk, K. and Sirviö, P. (2013). Polarization behavior of paper during corona charging. *Journal of Electrostatics*, 71, pp. 35–40.

Simula, S., Ikäläinen, S., Niskanen, K., Varpula, T., Seppä, H. and Pauku, A. (1999). Measurement of the dielectric properties of paper. *Journal of Imaging Science and Technology*, 43(5), pp. 472–477.

Sirviö, P., Sidaravicius, J., Lozovski, T., Kuskevicius, S. and K. Backfolk. (2009). Dosed charging: Application to the investigation of papers. *Journal of Electrostatics*, 67, pp. 730–736.

Smirnova, L. A., Narinskaya, A. R. and Smirnov, A. P. (1971). *Drying of fabrics with coatings based on aqueous dispersions of polymers*.

Staples, E. C., Greenwood, F., Brearley, W. and Woodhead, D. (1899). Improvements in or in connection with the water- and grease proofing of paper, packing papers, cardboard, and the like, and articles made therefrom, Patent GB189920667A, December 30.

Steward, P. A., Hearn, J. and Wilkinson M. C. (2000). An overview of polymer latex film formation and properties. *Advances in Colloid and Interface Science*, 86(3), pp. 195–267.

Strobel, M., Jones, V., Lyons, C. S., Ulsh, M., Kushner, M. J., Dorai, R. and Branch, M. C. (2003). A comparison of corona-treated and flame-treated polypropylene films. *Plasmas and Polymers*, 8(1), pp. 61–95.

Svanberg, L., Ahrné, L., Lorén, N. and Windhab, E. (2011). Effect of pre-crystallization process and solid particle addition on microstructure in chocolate model systems. *Food Research International*, 44(5), pp. 1339–1350.

Tanninen, P., Lindell, H., Saukkonen, E. and Backfolk, K. (2014). Thermal and mechanical stability of starch-based dual polymer coatings in the press forming of paperboard. *Packaging Technology and Science*, 29(5), pp. 353–363.

Tanninen, P., Saukkonen, E., Leminen, V., Lindell, H. and Backfolk, K. (2015). Adjusting the die cutting process and tools for biopolymer dispersion coated paperboards. *Nordic Pulp and Paper Research Journal*, 30(2), pp. 336–343.

Tuominen, M., Lahti, J., Lavonen, J., Penttinen, T., Räsänen, J. P. and Kuusipalo, J. (2010). The influence of flame, corona and atmospheric plasma treatments on surface properties and digital print quality of extrusion coated paper. *Journal of Adhesion Science and Technology*, 24(3), pp. 471–492.

Tuschhoff, J.V. (1986). Hydroxypropylated Starches. In: Wurtzburg O. B. Ed., *Modified Starches: Properties and Uses*, CRC Press, Inc., Boca Raton, Florida, USA, pp. 89–96.

Twede, D., Selke, S. E. M., Kamden, D.-P. and Shines, D. (2015). Types of paper, paperboard, laminates and adhesives. In: *Cartons, Crates and Corrugated Board*, DEStech Publications, Inc., Lancaster, Pennsylvania, USA, pp. 275–302.

Vander Wielen and L. C., Ragauskas, A. J. (2002). Corona discharge amplification of acid group topochemistry, *IPST Technical Paper Series Number 943*.

Vishtal, A. and Retulainen, E. (2012). Deep-drawing of paper and paperboard: The role of material properties. *Bioresources*, 7(3), pp. 4424–4450.

Viström, M. (2008). *Aspects of the Impact of Technology Integration on Agility and Supply Chain Management – the Potential of Digital Packaging Printing*, Dissertation, Lund University, Sweden. 110 p.

Vyörykkä, J., Zuercher, K. and Malotky, D. (2011). *Aqueous polyolefin dispersion for packaging board and papers*. In: TAPPI PaperCon Conference, Cincinnati, OH, USA, pp. 520–527.

Vähä-Nissi, M., Savolainen, A., Talja, M. and Mörö, R. (1998a). Dispersion barrier coating of high-density base papers. *TAPPI Journal*, 81(11), pp. 165–173.

Vähä-Nissi, M. (1998b). *HD Paper as Barrier Material*, Dissertation, Tampere University of Technology, Finland. 128 p.

Vähä-Nissi, M. and Savolainen, A. (1999). *Filled barrier dispersion coatings*. In: TAPPI Coating Conference, Toronto, ON, Canada. 17 p.

Vähä-Nissi, M., Taskinen, S.-M. and Savolainen, A. (2000). *Repulpability of dispersion-coated substrates*. In: TAPPI Coating Conference, Washington D. C., USA, pp. 151–161.

Vähä-Nissi, M., Lahti, J., Savolainen, A., Rissa, K. and Lepistö, T. (2001). New water-based barrier coatings for paper and paperboard. *Appita Journal*, 54(2), pp. 106–115.

Vähä-Nissi, M., Kervinen, K., Savolainen, A., Egolf, S. and Lau, W. (2006). Hydrophobic polymers as barrier dispersion coatings. *Journal of Applied Polymer Science*, 101, pp. 2958–2962.

Vähä-Nissi, M., Laine, C., Talja, R., Mikkonen, H., Hyvärinen, S. and Harlin, A. (2011). *Aqueous dispersions from biodegradable/renewable polymers*. In: TAPPI European Place Conference, Bregrens, Austria, pp. 1632–1660.

Väänänen, R., Heikkilä, P., Tuominen, M., Kuusipalo, J. and Harlin, A. (2010). Fast and efficient surface treatment for nonwoven materials by atmospheric pressure plasma. *AUTEX Research Journal*, 10(1), pp. 8–13.

Wenzel, R. N. (1936). Resistance of solid surfaces to wetting by water. *Industrial & Engineering Chemistry Research*, 28, pp. 988–994.

Wilbur, L. W. (1923). Greaseproofing composition of fibrous material treated thereby, US Patent 1454421A, May 8.

Wolf, R. A. (2007). *Troubleshooting corona treatment equipment on film extrusion lines*. In: 11th TAPPI European Place Conference, Athens, Greece. 2 p.

Wuu, F. and Rabot, Y. (2009). *High performance talc for water-based barrier coatings*. In: TAPPI PaperCon 2009, St. Louis, MO, USA, pp. 1841–1855.

Yeung, L. W. Y., So, M. K., Jiang, G., Taniyasu, S., Yamashita, N., Song, M., Wu, Y., Li, J., Giesy, J. P., Guruge, K. S. and Lam P. K. S. (2006). Perfluorooctanesulfonate and related fluorochemicals in human blood from China. *Environmental Science & Technology*, 40(3), pp. 715–720.

Zhao, Y. and McDaniel, M. (2005). Sensory quality of foods associated with edible film and coating systems and shelf-life extension. In: Han, J. H. Ed., *Innovations in Food Packaging*, Elsevier Academic Press, London, UK, pp. 434–453.

Zhu, Y. D., Allen, G. C., Adams, J. M., Gittins, D. I., Hooper, J. J. and Skuse, D. R. (2013). Barrier properties of latex/kaolin coatings. *Polymer Chemistry*, 4(16), pp. 4386–4395.

Zou, Y., Hsich, J. S., Mehnert, E. and Kokoszka, J. (2007). The effect of pigments and latices on the properties of coated paper. *Colloids and Surfaces A*, 294, pp. 40–45.

Publication I

Ovaska, S.-S., Geydt, P., Österberg, M., Johansson, L.-S. and Backfolk, K.
Heat-induced changes in oil and grease resistant hydroxypropylated-starch-based barrier coatings

Reprinted with permission from
Nordic Pulp and Paper Research Journal
Vol. 30, pp. 488–496, 2015
© 2004–2016 Nordic Pulp & Paper Research Journal

Publication II

Ovaska, S.-S., Hiltunen, S., Erntsson, M., Schuster, E., Altskär, A. and Backfolk, K.
**Characterization of rapeseed oil/coconut oil mixtures and their penetration into
hydroxypropylated-starch-based barrier coatings containing an oleophilic mineral**

Reprinted with permission from
Progress in Organic Coatings
Vol. 101, pp. 569–579, 2016
© 2016 Progress in Organic Coatings

Publication III

Ovaska, S.-S., Mielonen, K., Lozovski, T., Rinkunas, R., Sidaravicius, J. and Backfolk, K.
A novel approach for studying the effects of corona treatment on ink-substrate interactions

Reprinted with permission from
Nordic Pulp and Paper Research Journal
Vol. 30, pp. 681–688, 2015
© 2004–2016 Nordic Pulp & Paper Research Journal

Publication IV

Ovaska, S.-S., Rinkunas, R., Lozovski, T., Maldzius, R., Sidaravicius, J., Österberg, M.,
Johansson, L.-S. and Backfolk, K.

**Corona treatment of filled dual-polymer dispersion coatings: Surface properties and grease
resistance**

Accepted to *Polymers & Polymer Composites* in March 2016

Publication V

Ovaska, S.-S., Rinkunas, R., Lozovski, T., Sidaravicius, J., Österberg, M., Johansson, L.-S.,
Maldzius, R. and Backfolk, K.

**Occurrence of reverse side effects in corona treatment of dispersion-coated paperboard
and its influence on grease barrier properties**

Reprinted with permission from
Journal of Applied Packaging Research
Vol. 8, issue 3, pp. 68–79, 2016

Publication VI

Leminen, V., Ovaska, S.-S., Tanninen, P. and Varis, J.

Convertability and oil resistance of paperboard with hydroxypropyl-cellulose-based dispersion barrier coatings

Reprinted with permission from
Journal of Applied Packaging Research
Vol. 7, issue 3, pp. 91–100, 2015

ACTA UNIVERSITATIS LAPPEENRANTAENSIS

681. VALTONEN, PETRI. Distributed energy resources in an electricity retailer's short-term profit optimization. 2015. Diss.
682. FORSSTRÖM-TUOMINEN, HEIDI. Collectiveness within start up-teams – leading the way to initiating and managing collective pursuit of opportunities in organizational contexts. 2015. Diss.
683. MAGUYA, ALMASI. Use of airborne laser scanner data in demanding forest conditions. 2015. Diss.
684. PEIPPO, JUHA. A modified nominal stress method for fatigue assessment of steel plates with thermally cut edges. 2015. Diss.
685. MURASHKO, KIRILL. Thermal modelling of commercial lithium-ion batteries. 2016. Diss.
686. KÄRKKÄINEN, TOMMI. Observations of acoustic emission in power semiconductors. 2016. Diss.
687. KURVINEN, EMIL. Design and simulation of high-speed rotating electrical machinery. 2016. Diss.
688. RANTAMÄKI, JUKKA. Utilization of statistical methods for management in the forest industry. 2016. Diss.
689. PANOVA, YULIA. Public-private partnership investments in dry ports – Russian logistics markets and risks. 2016. Diss.
690. BAHARUDIN, EZRAL. Real-time simulation of multibody systems with applications for working mobile vehicles. 2016. Diss.
691. MARTIKAINEN, SOILI. Development and effect analysis of the Asteri consultative auditing process – safety and security management in educational institutions. 2016. Diss.
692. TORVINEN, PEKKA. Catching up with competitiveness in emerging markets – An analysis of the role of the firm's technology management strategies. 2016. Diss.
693. NORONTAUS, ANNUKKA. Oppisopimuskoulutus yritysten tuottamana koulutuspalveluna: tavoitteista vaikutuksiin. 2016. Diss.
694. HALMINEN, OSKARI. Multibody models for examination of touchdown bearing systems. 2016. Diss.
695. TALONPOIKA, ANNA-MARIA. Financial working capital – management and measurement. 2016. Diss.
696. INKINEN, HENRI. Intellectual capital, knowledge management practices and firm performance. 2016. Diss.
697. YANG, XIAOCHEN. Development of a welding production quality control and management system model for China. 2016. Diss.
698. LEMINEN, VILLE. Leak-proof heat sealing of press-formed paperboard trays. 2016. Diss.

699. LAAKSONEN, LAURI. Spectral retinal image processing and analysis for ophthalmology. 2016. Diss.
700. OINONEN, MINNA. Management of customer co-development in business-to-business markets. 2016. Diss.
701. ALATALO, SARA-MAARIA. Hydrothermal carbonization in the synthesis of sustainable porous carbon materials. 2016. Diss.
702. UZHEGOV, NIKITA. Design and material selection of high-speed rotating electrical machines. 2016. Diss.
703. RICHTER, CHRIS. Digital collaborations and entrepreneurship – the role of shareconomy and crowdsourcing in the era of smart city. 2016. Diss.
704. JAFARI, SHILA. Investigation of adsorption of dyes onto modified titanium dioxide. 2016. Diss.
705. PATEL, YOGINI. Computational modelling of non-equilibrium condensing steam flows in low-pressure steam turbines. 2016. Diss.
706. LEVCHUK, IRINA. Titanium dioxide based nanomaterials for photocatalytic water treatment. 2016. Diss.
707. AMOUR, IDRISSE. Variational ensemble kalman filtering applied to data assimilation problems in computational fluid dynamics. 2016. Diss.
708. SHESTAKOVA, MARINA. Ultrasound-assisted electrochemical treatment of wastewaters containing organic pollutants by using novel Ti/Ta₂O₅-SnO₂ electrodes. 2016. Diss.
709. OLEKSIENKO, OLGA. Physico-chemical properties of sol-gel synthesized titanosilicates for the uptake of radionuclides from aqueous solutions. 2016. Diss.
710. PATALA, SAMULI. Advancing sustainability-oriented innovations in industrial markets. 2016. Diss.
711. KUORIKOSKI, TERO. Kohti resonoivaa urheilujohtamista – Tavoitteen muodostuminen urheilun kentässä. 2016. Diss.
712. LAHTELA, VILLE. Improving the properties of solid Scots pine (*Pinus sylvestris*) wood by using modification technology and agents. 2016. Diss.
713. NEVARANTA, NIKO. Online time and frequency domain identification of a resonating mechanical system in electric drives. 2016. Diss.
714. FANG, CHAO. Study on system design and key technologies of case closure welding for ITER correction coil. 2016. Diss.
715. GARCÍA PÉREZ, MANUEL. Modeling the effects of unsteady flow patterns on the fireside ash fouling in tube arrays of kraft and coal-fired boilers.
716. KATTAINEN, JARI. Heterarkkisen verkostoyhteistyön johtamistarpeet verkoston muotoutumisvaiheessa. 2016. Diss.
717. HASAN, MEHDI. Purification of aqueous electrolyte solutions by air-cooled natural freezing. 2016. Diss.
718. KNUTAS, ANTTI. Increasing beneficial interactions in a computer-supported collaborative environment. 2016. Diss.

